

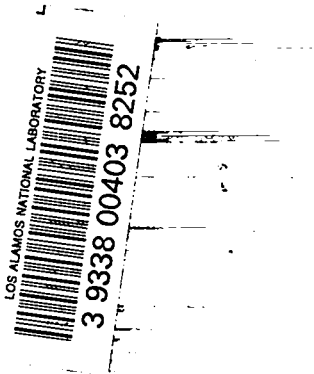
C.3

LA-3279

CIC-14 REPORT COLLECTION
**REPRODUCTION
COPY**

LOS ALAMOS SCIENTIFIC LABORATORY
LOS ALAMOS ██████████ of the ██████████ NEW MEXICO
University of California

**ULTRA HIGH TEMPERATURE REACTOR
CRITICAL EXPERIMENT (UCX)
SAFETY ANALYSIS REPORT**



**UNITED STATES
ATOMIC ENERGY COMMISSION
CONTRACT W-7405-ENG. 36**

LEGAL NOTICE

This report was prepared as an account of Government sponsored work. Neither the United States, nor the Commission, nor any person acting on behalf of the Commission:

A. Makes any warranty or representation, expressed or implied, with respect to the accuracy, completeness, or usefulness of the information contained in this report, or that the use of any information, apparatus, method, or process disclosed in this report may not infringe privately owned rights; or

B. Assumes any liabilities with respect to the use of, or for damages resulting from the use of any information, apparatus, method, or process disclosed in this report.

As used in the above, "person acting on behalf of the Commission" includes any employee or contractor of the Commission, or employee of such contractor, to the extent that such employee or contractor of the Commission, or employee of such contractor prepares, disseminates, or provides access to, any information pursuant to his employment or contract with the Commission, or his employment with such contractor.

Printed in USA. Price \$4.00. Available from the

Clearinghouse for Federal Scientific
and Technical Information,
National Bureau of Standards,
U. S. Department of Commerce,
Springfield, Virginia

LA-3279
UC-80, REACTOR TECHNOLOGY
TID-4500 (38th Ed.)

LOS ALAMOS SCIENTIFIC LABORATORY
LOS ALAMOS  **of the**  **NEW MEXICO**
University of California

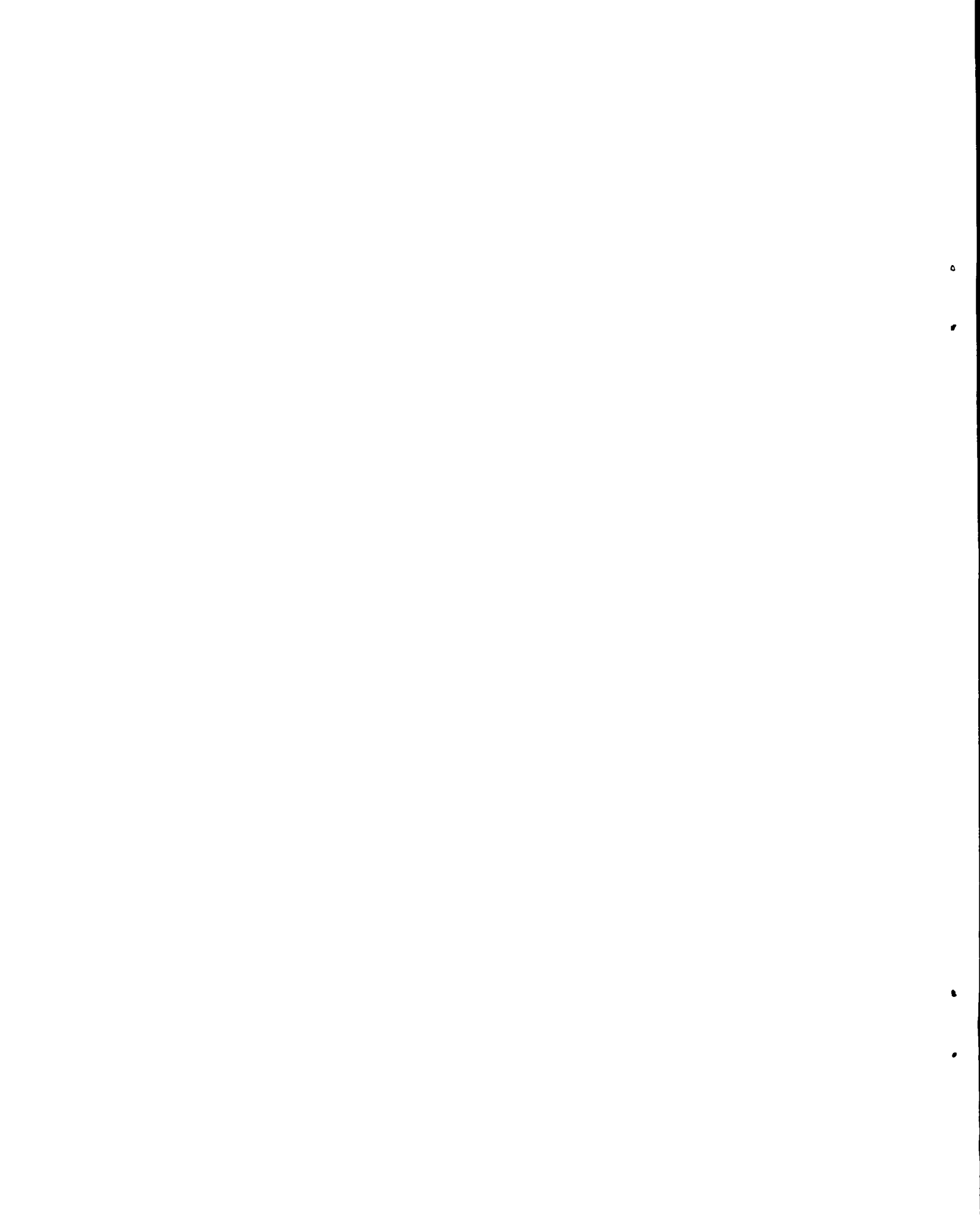
Report written: March 1965

Report distributed: March 31, 1965

ULTRA HIGH TEMPERATURE REACTOR
CRITICAL EXPERIMENT (UCX)
SAFETY ANALYSIS REPORT

Prepared By
K-Division



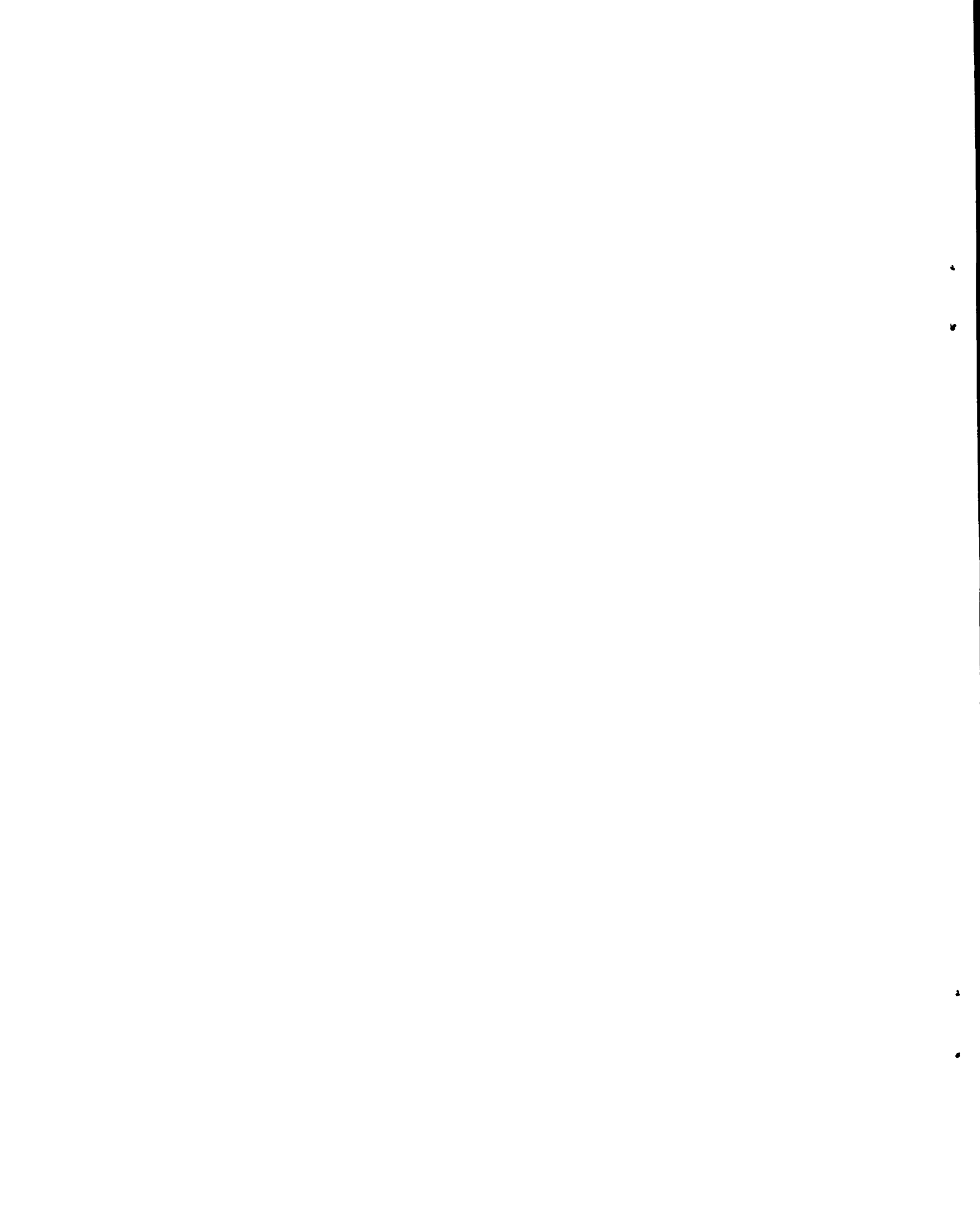


ABSTRACT

The UHTREX Critical Experiment uses the core, reflector, fuel elements, and control rod materials of UHTREX to produce data for the verification of nuclear design calculations.

Components of the critical assembly and the plans for its operation are described and discussed, as are the location and design features of the test facility.

Hazards that might arise during UCX operation are described and the consequences analyzed. Consequences of conceivable excursions are minor, with effects limited to the assembly test cell.



CONTENTS

| | Page |
|--------------------------------------|------|
| 1. Introduction | 8 |
| 1.1 Summary | 8 |
| 1.2 Conclusions | 9 |
| 2. Site Information | 11 |
| 2.1 Location | 11 |
| 2.2 Layout | 11 |
| 2.3 Population | 14 |
| 2.4 Meteorology | 14 |
| 2.4.1 Winds | 14 |
| 2.4.2 Inversions | 18 |
| 2.4.3 Precipitation and Temperatures | 20 |
| 2.5 Hydrology and Geology | 20 |
| 2.6 Seismicity | 20 |
| 3. Facility | 22 |
| 3.1 General Description | 22 |
| 3.2 Pit Building (TSL-29) | 22 |
| 3.2.1 Reactor Test Pit | 27 |
| 3.2.2 High Bay | 27 |
| 3.2.3 Terminal Room | 30 |
| 3.2.4 Cell Access Room and Corridor | 30 |
| 3.3 Tunnel (TSL-35) | 32 |
| 3.4 Control Room Area (TSL-26) | 32 |
| 3.4.1 Control Room | 32 |
| 3.4.2 Basement and Mezzanine | 32 |
| 3.5 Shielding | 33 |
| 3.5.1 Neutron Shielding Calculations | 33 |
| 3.5.2 Gamma Shielding Calculations | 33 |
| 3.5.3 Conclusions | 38 |

CONTENTS (continued)

| | Page |
|---|------|
| 3.6 Utilities | 38 |
| 3.6.1 Electrical Power | 38 |
| 3.6.2 Communications Systems | 39 |
| 3.6.3 Fire Protection System | 39 |
| 3.6.4 Sump System | 40 |
| 3.7 Health Physics Instrumentation | 40 |
| 3.8 Ventilation | 41 |
| 3.8.1 Test Pit | 41 |
| 3.8.2 Access and High Bay Areas | 41 |
| 4. Experiment | 43 |
| 4.1 Critical Assembly | 43 |
| 4.1.1 Core | 43 |
| 4.1.2 Fuel Elements | 49 |
| 4.1.3 Control Rods | 52 |
| 4.1.4 Control Rod Drives | 54 |
| 4.1.5 Startup Source | 56 |
| 4.1.6 Nuclear Instrumentation | 56 |
| 4.1.7 Non-Nuclear Instrumentation | 59 |
| 4.2 Nuclear Operations | 59 |
| 4.2.1 Determination of Cold Critical Loading (Phase I) | 60 |
| 4.2.2 Initial Control Rod Calibration (Phase I) | 65 |
| 4.2.3 Power Profile Measurement (Phase I) | 65 |
| 4.2.4 Measurement of Temperature Coefficient (Phase I) | 65 |
| 4.2.5 Source Experiments (Phase I) | 66 |
| 4.2.6 Measurement of the Reactivity Effect of Unloaded Graphite and Void (Phase I) | 67 |
| 4.2.7 Evaluation of Control Rod System (Phase II) | 67 |

CONTENTS (continued)

| | Page |
|---|------|
| 5. Safeguards | 69 |
| 5.1 Administration | 69 |
| 5.2 Initial Facility Checkout and Preoperational Tests | 69 |
| 5.2.1 Control Rod Drives | 69 |
| 5.2.2 Source Actuator | 69 |
| 5.2.3 Nuclear Instrumentation | 70 |
| 5.3 Procedural Controls | 70 |
| 5.3.1 Operating Limits | 70 |
| 5.3.2 Area Control | 71 |
| 5.3.3 Emergencies | 71 |
| 5.3.4 Maintenance | 71 |
| 5.4 Interlocks | 72 |
| 6. Hazards | 73 |
| 6.1 Inherent Safety of the Core | 73 |
| 6.2 Reactivity Addition by Rod Withdrawal | 74 |
| 6.2.1 Case I: Available Reactivity Is 90¢ | 75 |
| 6.2.2 Case II: Available Reactivity Is Greater Than 90¢ | 77 |
| 6.3 Reactivity Increases through Mechanical Changes to the Assembly | 79 |
| 6.4 Reactivity Addition during Fuel Loading | 80 |
| Appendices | |
| A. Meteorological Data for Los Alamos | 81 |
| B. Geology and Hydrology of the TA-35 Site | 86 |
| C. UCX Nuclear Safety System | 88 |
| D. Hazard Analyses | 94 |

1. INTRODUCTION

As a preliminary to the Ultra High Temperature Reactor Experiment, the Los Alamos Scientific Laboratory will perform the UHTREX Critical Experiment. For UCX, the graphite core, the graphite and carbon reflector, the fuel elements, and close simulations of the control rods of the UHTREX reactor ¹ are used in a series of experiments planned to produce data for the verification of the nuclear calculations upon which the design of UHTREX is based.

1.1 Summary

Within the reactor test cell complex at the TA-35 technical area of LASL, the graphite and carbon parts of the UHTREX core and reflector are assembled with a drive mechanism that rotates the movable core. Mounted on top of the reflector, an aluminum superstructure supports five control rod drives and a neutron source actuator, all remotely controlled. The small, cylindrical UHTREX fuel elements are loaded singly with a hand tool into the core, through the fuel loader slot in the reflector, and discharge, through the core plug exit slot, into a wheeled, padded box from which the elements are removed manually. Control rods, nearly identical in nuclear properties to the UHTREX rods, are contained in rigid aluminum tubes. Fourteen

1. "Ultra High Temperature Reactor Experiment (UHTREX) Hazard Report," LA-2689, March, 1962.

instrument channels collect nuclear data from the assembly and transmit to a remotely-located control room, from which all nuclear operations are controlled.

The critical experiment is planned in two phases. In phase I, the following experiments are performed while an excess reactivity of less than $\$1$ is available in the reactor:

1. Determination of the cold critical core loading,
2. Control rod calibration within the excess reactivity limits,
3. Measurements of the core's power profile,
4. Measurement of the near-ambient temperature coefficient of reactivity,
5. Investigation of the effect on measured neutron multiplication of neutron source-detector geometry, and
6. Measurement of the reactivity effect of voids or unloaded graphite in the place of fuel.

Phase II experiments complete the calibration of all sixteen control rods.

1.2 Conclusions

The UHTREX Critical Experiment is located in a facility that will prevent any external radiation hazard during the most extreme excursion that can occur. Because UCX operates at very low power levels, no significant fission product inventory will accumulate. Therefore, there is no off-site hazard.

At all times the core is so well reflected, by a heavy graphite reflector, that external reflection produces no significant change in assembly reactivity. The structures of the core and reflector optimize moderation to such an extent that, if the assembly were flooded with water, reactivity would be decreased.

Reactivity additions by control rod movement at the maximum available rates produce limited excursions that do no damage to the assembly, the facility, or to personnel in the vicinity. The production of a power transient by hand loading of the small fuel elements, each worth 2 or 3ç, would be difficult, even if procedures were ignored and precautions were nullified. Accidents that cause mechanical damage to the core, sufficient to alter its configuration, would produce little increase in reactivity.

The critical experiment will be performed in consonance with the proposed "Code of Good Practices for the Performance of Critical Experiments," prepared by Sub-Committee ANS-1 of the American Nuclear Society Standards Committee. Written experimental plans, reviewed and approved by the UHTREX Planning Committee, will govern all operations that result in a multiplication greater than 10. The experimental plans will describe proposed activities and prescribe operating procedures.

2. SITE INFORMATION

2.1 Location

The UHTREX Critical Experiment will be conducted at TA-35, located within a Los Alamos area owned and controlled by the Atomic Energy Commission. The TA-35 site is approximately two miles southeast of the city of Los Alamos (see Fig. 2.1.1), 15 miles southwest of Espanola, and 22 miles northwest of Santa Fe. Most of the Los Alamos Scientific Laboratory technical areas and much of the Los Alamos residential area lie within a three-mile radius of TA-35. The nearest residential area is 3/4 mile distant.

2.2 Layout

TA-35 (also known as "Ten Site") is located on a narrow mesa shown in Fig. 2.2.1. The experiment will be conducted in the Test Pit Building, TSL-29, which is located among other structures within a fenced area to which access is restricted to persons on official business. To the south of TSL-29 is a filter building which serves the plutonium laboratories and is occupied only intermittently by maintenance personnel. On the west side are TSL-2 and TSL-26, the K-Division laboratory and office buildings, in full use during normal office hours. Outside the security fence to the northeast is the site of the Fast Reactor Core Test Facility, now under construction. The construction site, which comes within 10 feet of the north wall of TSL-29, is open to a 50-man construction crew and to casual visitors during work hours. Members of the contractor's supervisory force can enter the job site at any time.

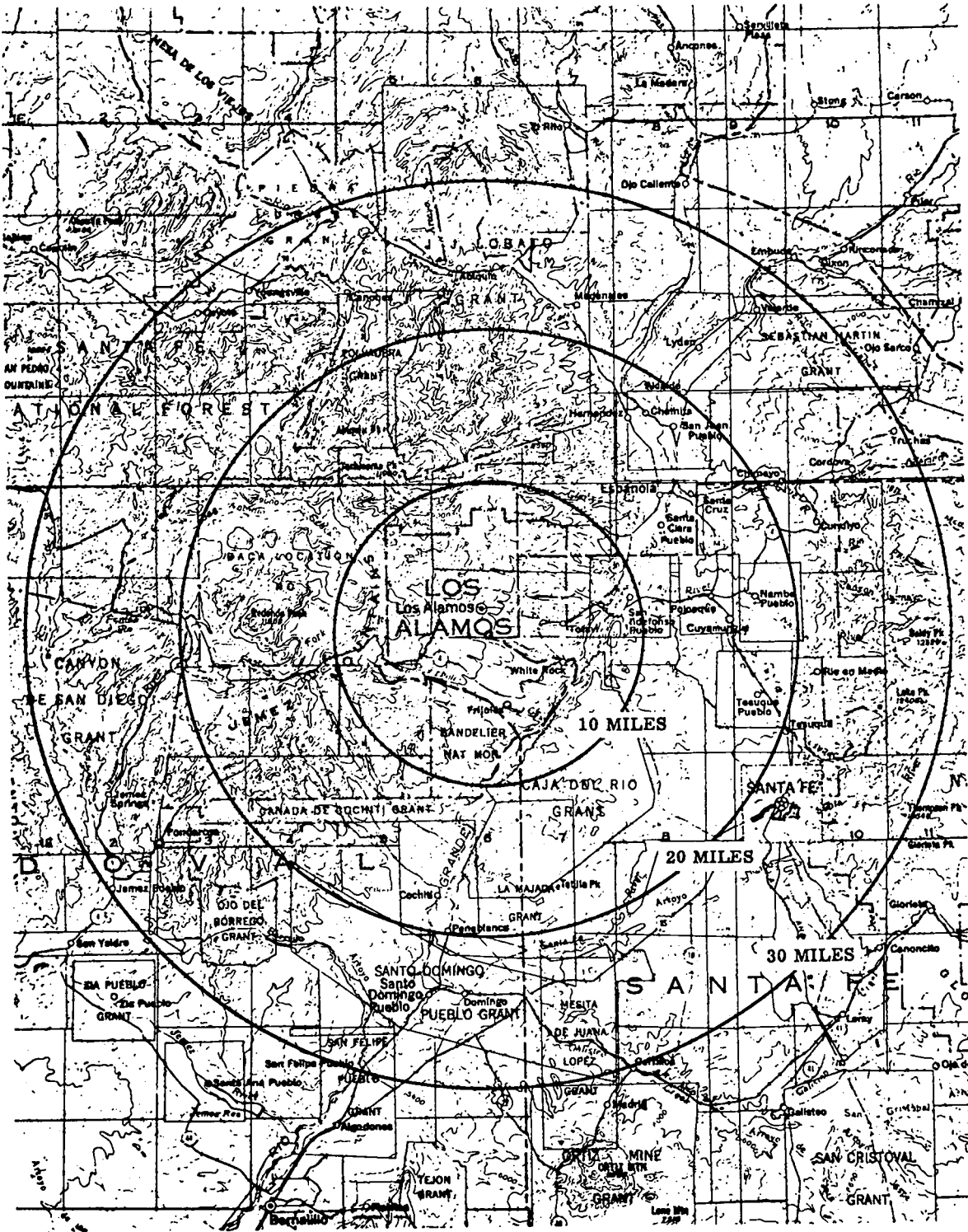


Fig. 2.1.1. Map of area surrounding Los Alamos.

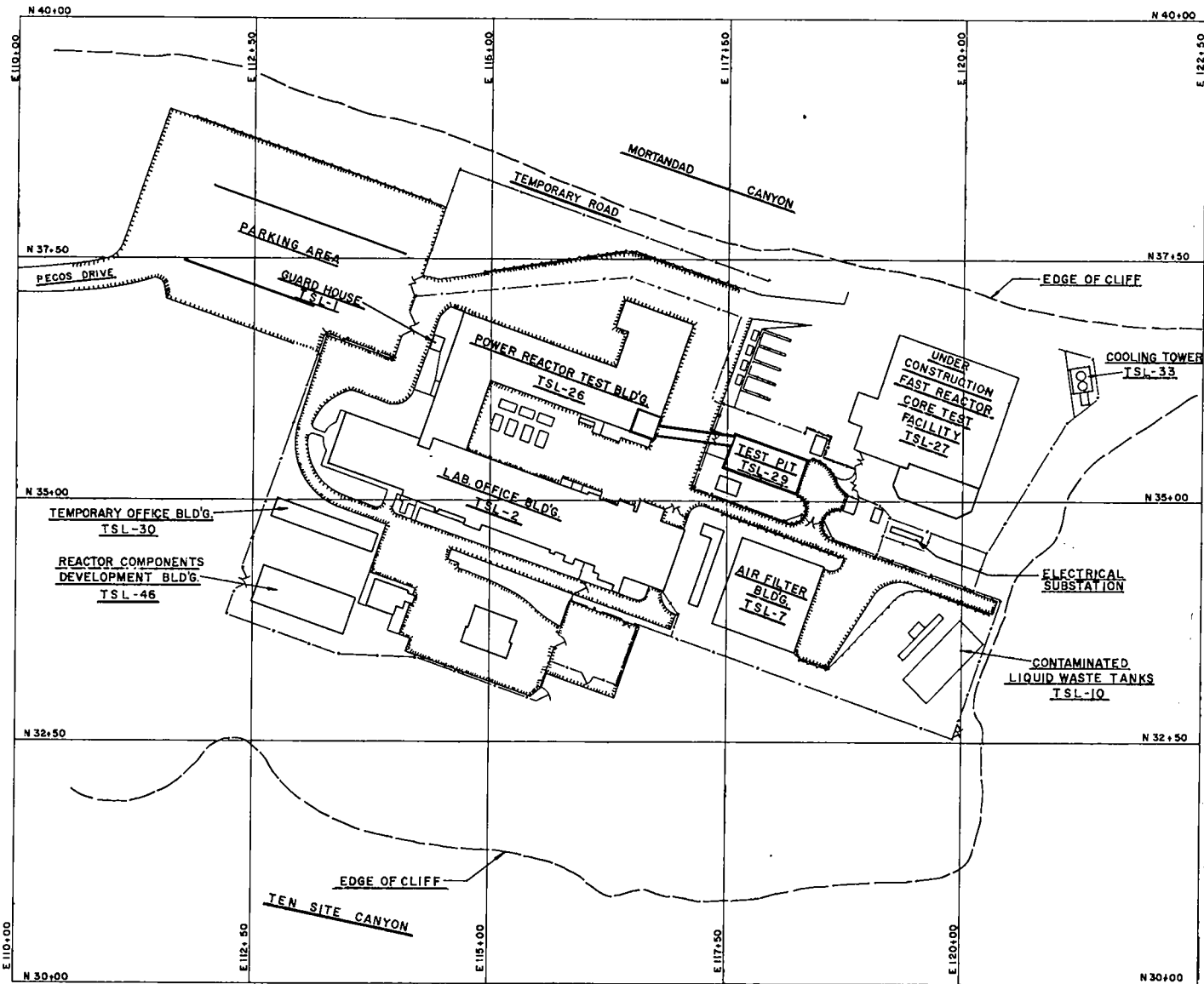


Fig. 2.2.1 Map of TA-35 Site.

2.3 Population

The population in the vicinity of TA-35 is concentrated inside the LASL technical areas and within the city of Los Alamos. Figure 2.3.1 shows the population distribution for both technical and residential areas, and Table 2.3.1 lists the names and uses of the various technical area sites. Table 2.3.2 summarizes the population distribution by radial zones. The numbers are not additive, because 75 percent of the people listed for the technical areas are also counted for the residential areas. During working hours, there are a total of 16,500 people in the Los Alamos area.

Except for the city of Los Alamos, the area within a 10-mile circle of TA-35 is sparsely populated. There are a few permanent residents at Frijoles, five miles SSE; but during the summer, visitors to the Bandelier National Monument can raise the population to nearly 300. White Rock, five miles ESE, has a population of 850. At San Ildefonso Pueblo, nine miles to the ENE, there are approximately 400 people.

In the 10-20-mile zone, the total population is 12,000, with 8,000 concentrated around Espanola, 15 miles to the northeast.

Between 20 and 30 miles away from the site, the total population is almost 40,000, with 85 percent of the people concentrated in the vicinity of Santa Fe, 22 miles to the southeast.

There are no other population centers within 50 miles of the site. Albuquerque, population 300,000, lies 53 miles to the south.

2.4 Meteorology

2.4.1 Winds

Surface movements of air at the TA-35 site are influenced strongly by its location on a mesa that slopes away from the Jemez Mountains on the west. The site is surrounded on the other three sides

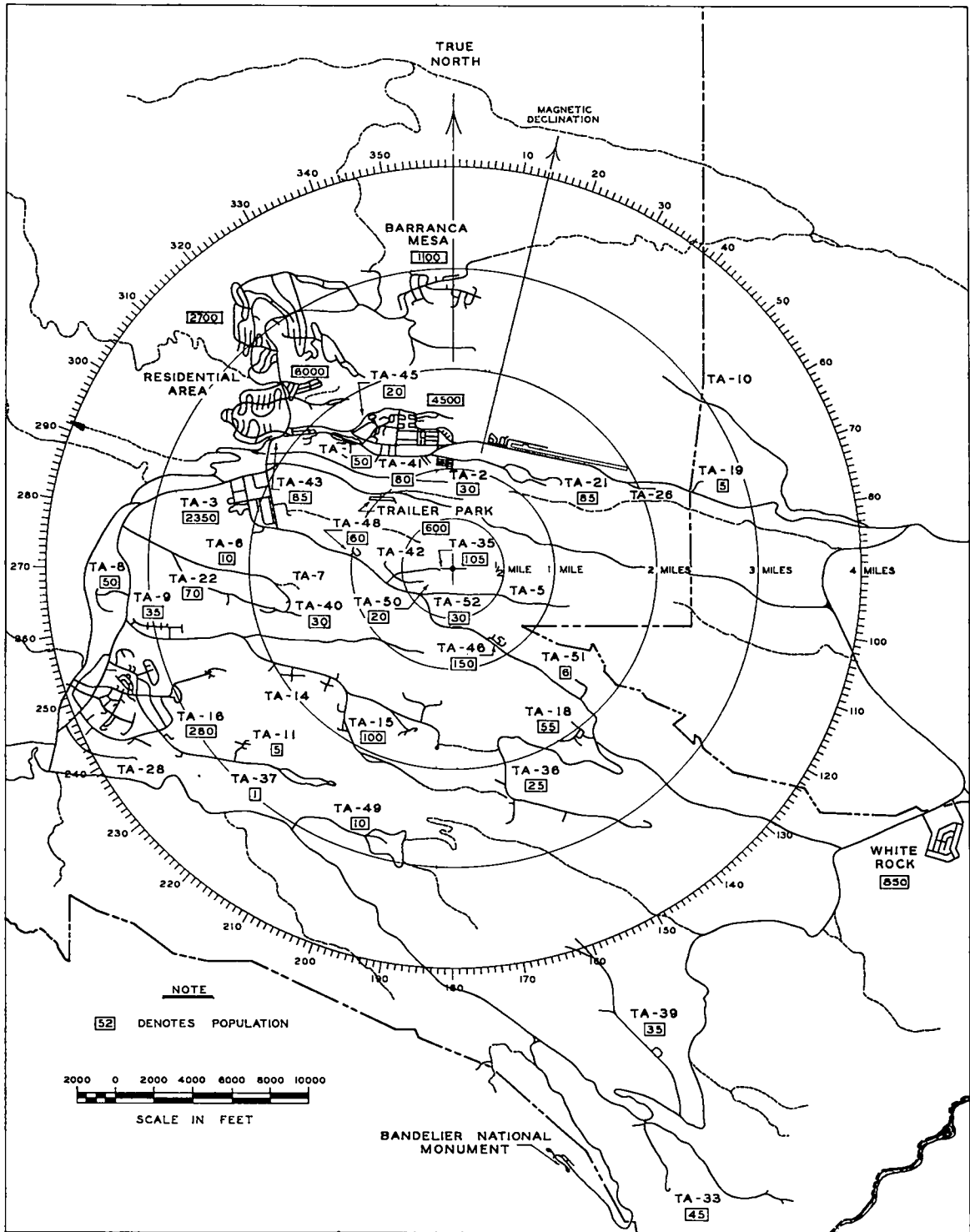


Fig. 2.3.1. Map of Los Alamos residential and technical areas. Boxes show local area population.

TABLE 2.3.1
LASL TECHNICAL AREAS

| <u>Technical Area Number</u> | <u>Name</u> | <u>Facilities and Functions</u> |
|------------------------------|---------------------------------------|--|
| TA-1 | Former Main Technical Area | Being razed |
| TA-2 | Omega Site | OWR, Water Boiler Reactor, offices, laboratories |
| TA-3 | South Mesa Site (Main Technical Area) | Offices, laboratories, shops |
| TA-5* | Beta Site | Laboratories |
| TA-6 | Two-Mile Mesa Laboratory | Offices, laboratories |
| TA-7* | Gomez Ranch Site | Abandoned |
| TA-8 | Anchor Site West | Offices, laboratories, sources for radiography |
| TA-9 | Anchor Site East | Offices, laboratories |
| TA-10 | Bayo Canyon | Abandoned |
| TA-11 | K-Site | Explosive testing |
| TA-14 | Q-Site | Explosive firing |
| TA-15 | R-Site | Offices, laboratories, explosive firing |
| TA-16 | S-Site | Offices, laboratories, explosive plant |
| TA-18 | Pajarito Laboratory | Offices, laboratories, critical assemblies |

* Sites used occasionally, by fewer than 10 persons.

TABLE 2.3.1 (continued)

| | | |
|---------|--------------------------------------|---|
| TA-21 | DP-Site | Offices, laboratories |
| TA-22 | TD-Site | Offices, laboratories, explosive plant |
| TA-26* | D-Site | Storage |
| TA-28* | Magazine Area A | Explosive Storage |
| TA-35 | Ten Site | Offices, laboratories, reactor development tests |
| TA-36 | Kappa Site | Offices, laboratories, explosive firing |
| TA-37 | Magazine Area C (PMA) | Explosive storage |
| TA-40 | DF-Site | Offices, laboratories, explosive firing |
| TA-41 | W-Site | Offices, laboratories |
| TA-42* | Incinerator Site | Incinerator |
| TA-43 | Health Research Laboratory | Offices, laboratories |
| TA-45 | WD-Site | Abandoned |
| TA-46 | WA-Site | Offices, laboratories |
| TA-48 | Radiochemistry Site | Offices, laboratories |
| TA-49 | Frijoles Mesa Site | Laboratories |
| TA-50 | Liquid Waste Plant | Offices, laboratories |
| TA-51 | Radiation Exposure Facility | Laboratories |
| TA-52 | Reactor Development Site | UHTREX |
| TA-53** | Los Alamos Meson Physics Facility | Offices, laboratories |

* Sites used occasionally, by fewer than 10 persons.

** Preliminary Design

TABLE 2.3.2

POPULATION WITHIN RADIAL ZONES

| <u>Zone Limits (Miles)</u> | <u>Los Alamos Areas Included</u> | <u>Number of People</u> |
|--------------------------------|--|-----------------------------|
| 0 - 0.5 | Technical Areas | 155 |
| 0.5- 1.0 | Technical Areas | 540 |
| 1.0- 2.0 | Residential and Central Business District Technical Areas | 4800 350 |
| 2.0- 3.0 | Residential Technical Areas | 6000 2500 |
| 3.0- 6.0 | Residential Technical Areas | 4650 445 |

by deep canyons that drain eastward into the Rio Grande Valley, 1500 ft below. After sunset, cooler air from the mountains flows across the mesas and channels through the canyons to the river valley. The flow is reversed during the day.

Winds are generally light and southerly. The average wind speed is less than 10 mph about 75 percent of the time and reaches 30 mph only 0.1 percent of the time, usually in gusts. Over the entire year, average wind direction lies in the quadrant from south to west about 50 percent of the time. Wind roses for 0600 and 1200, based on data from 11 years' observations, are shown in Fig. 2.3.2. Tabulations of average wind direction and speed for each month of the year are presented in Tables A.1 and A.2 of Appendix A.

2.4.2 Inversions

In the Los Alamos area, inversions are almost always caused by surface cooling or frontal activity. Surface cooling inversions, by

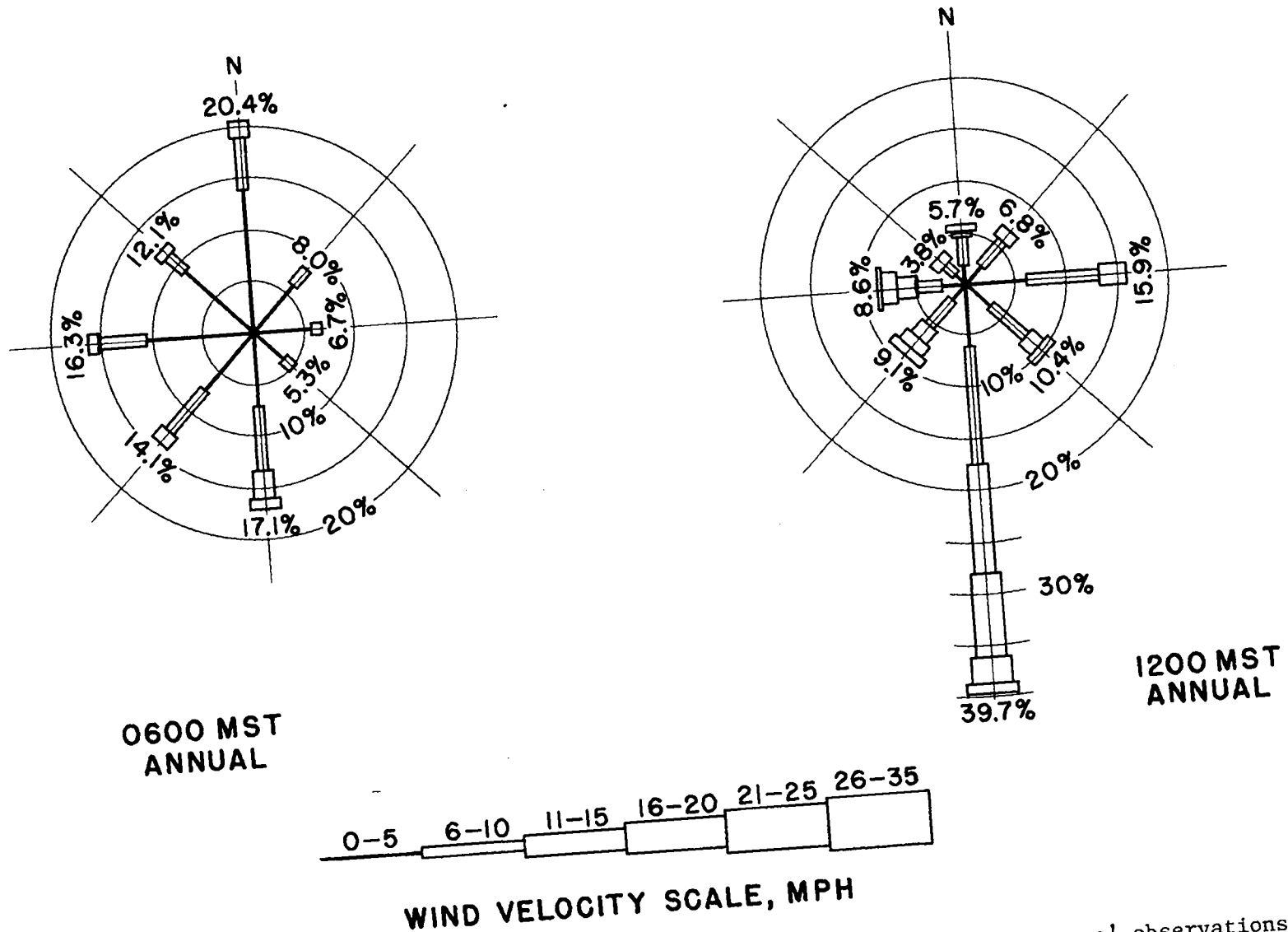


Fig. 2.3.2. Surface wind roses for Los Alamos based on data from eleven years' observations. Directions are those from which the wind blows.

far the most common, can be expected to form during any night when the skies are generally clear and wind speeds are low. On the mesas, such inversions usually dissipate by mid-morning. Inversions due to frontal activity are subject to considerable mixing caused by the moderate winds that usually accompany the fronts. Lateral mixing is reinforced by vertical mixing created by the mechanical turbulence of the winds flowing across the broken terrain.

2.4.3 Precipitation and Temperatures

Average precipitation and temperature data for Los Alamos are presented in Tables A.3 and A.4 of Appendix A.

2.5 Hydrology and Geology

Theis¹ has described the hydrology and geology of the Los Alamos area. A discussion by W. E. Hale is included in Appendix B.

2.6 Seismicity

The Los Alamos area is on the Rio Grande structural trough near faults of large magnitude, and hence, according to Hale, earthquakes might be expected to occur at any time. Further, the Los Alamos area might experience tremors from quakes originating in other parts of the trough. However, Hale continues, there is no geologic evidence to indicate that intensive earthquakes have occurred recently in the Los Alamos region.

According to S. A. Northrup,² in a region like New Mexico that is subject to a high frequency of shocks of moderate intensity, the

1 C. V. Theis, "Geologic Background of Waste and Water Supply Problems at Los Alamos," Paper No. 1, "Meeting of AEC Waste Processing Committee at Los Alamos, New Mexico," TID-460, October, 1950.

2 Collaborator in Seismology for New Mexico, U.S. Coast and Geodetic Survey; and Head, Department of Geology, University of New Mexico.

frequent shocks act as a safety valve to relieve earth stress before it can accumulate to produce a violent shock. Northrup reports that of 575 earthquakes recorded in New Mexico during the century preceding 1949, 94 percent originated in a 75-mile section of the Rio Grande Valley extending south from Albuquerque (53 miles south of Los Alamos) to Socorro. Only 2 percent of these shocks were of intensity VIII to IX on the Rossi-Forel scale. (Intensity I is a microseismic shock; intensity X is a shock that causes general disaster.) One of the strongest shocks, reported to be of intensity IX, originated near Cerrillos, 30 miles south of Los Alamos, on May 28, 1918. The resultant shock at Los Alamos presumably attained intensity VI or, with remote possibility, intensity VII. Another report³ lists a brief shock of intensity V that occurred at Los Alamos on August 17, 1952.

³ "Abstracts of Earthquake Reports for the Pacific Coast and the Western Mountain Region," MSA-75, July, August, and September, 1952, U.S. Coast and Geodetic Survey.

3. FACILITY

3.1 General Description

The reactor test cell complex was constructed to provide a place where criticality experiments can be performed with a wide variety of reactor cores at modest power levels. Installed control and power cables, ventilation and utility service systems, a supply of portable shielding for supplementary use, and a control room located at a distance from the core test pit, were designed for versatility in operation of the facility. Many of the facilities features, e.g., the pit liner and the ventilation system, were designed specifically to accommodate experiments with plutonium alloy-fueled cores. These features are not relevant to UCX, but are included for clarity in the facility descriptions.

Three structures at TA-35 contain the reactor test cell complex: The pit building (TSL-29); the control room and its basement, in the north wing of the main K-Division Office and laboratory building (TSL-26); and an 80-foot connecting tunnel (TSL-35). The physical arrangement of the complex is shown in Fig. 3.1.1.

3.2 Pit Building (TSL-29)

An above-grade, single-bay structure and three levels that extend to 25 ft below grade make up the pit building. Plans of the building at the 0 ft level (grade level), -15 ft level, and -25 ft level are presented in Fig. 3.2.1, 3.2.2, and 3.2.3.

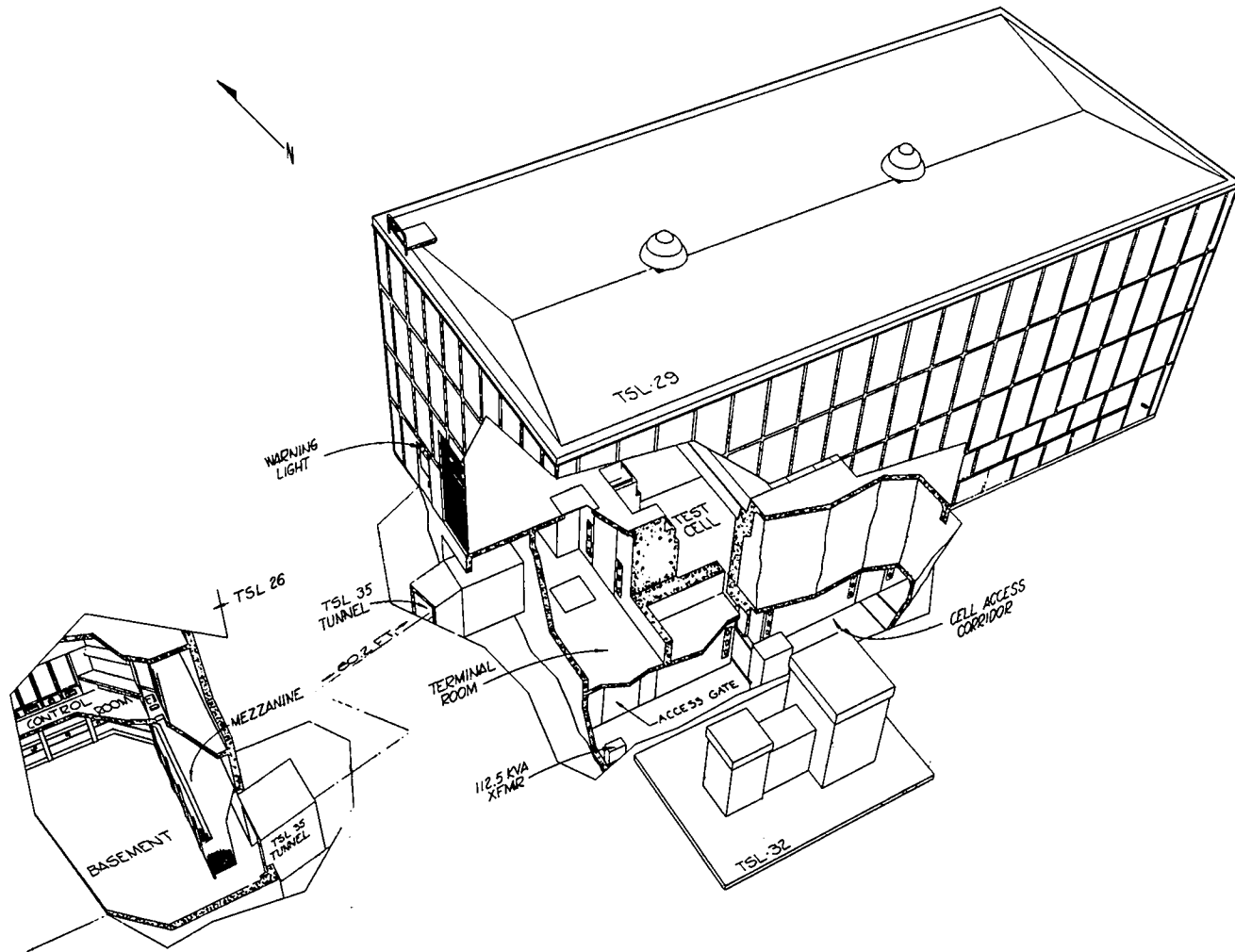


Fig. 3.1.1. Isometric view of reactor test cell complex.

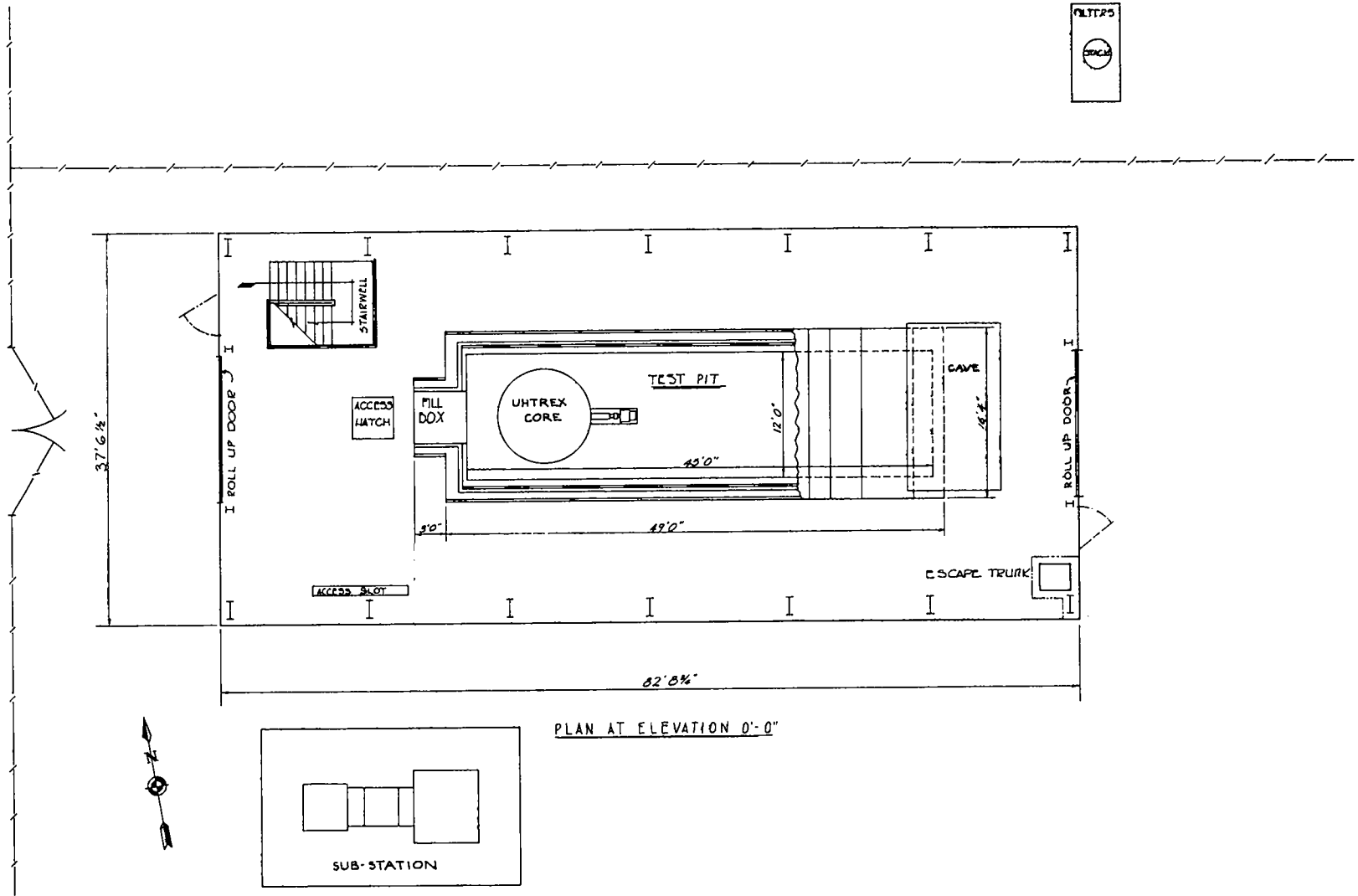
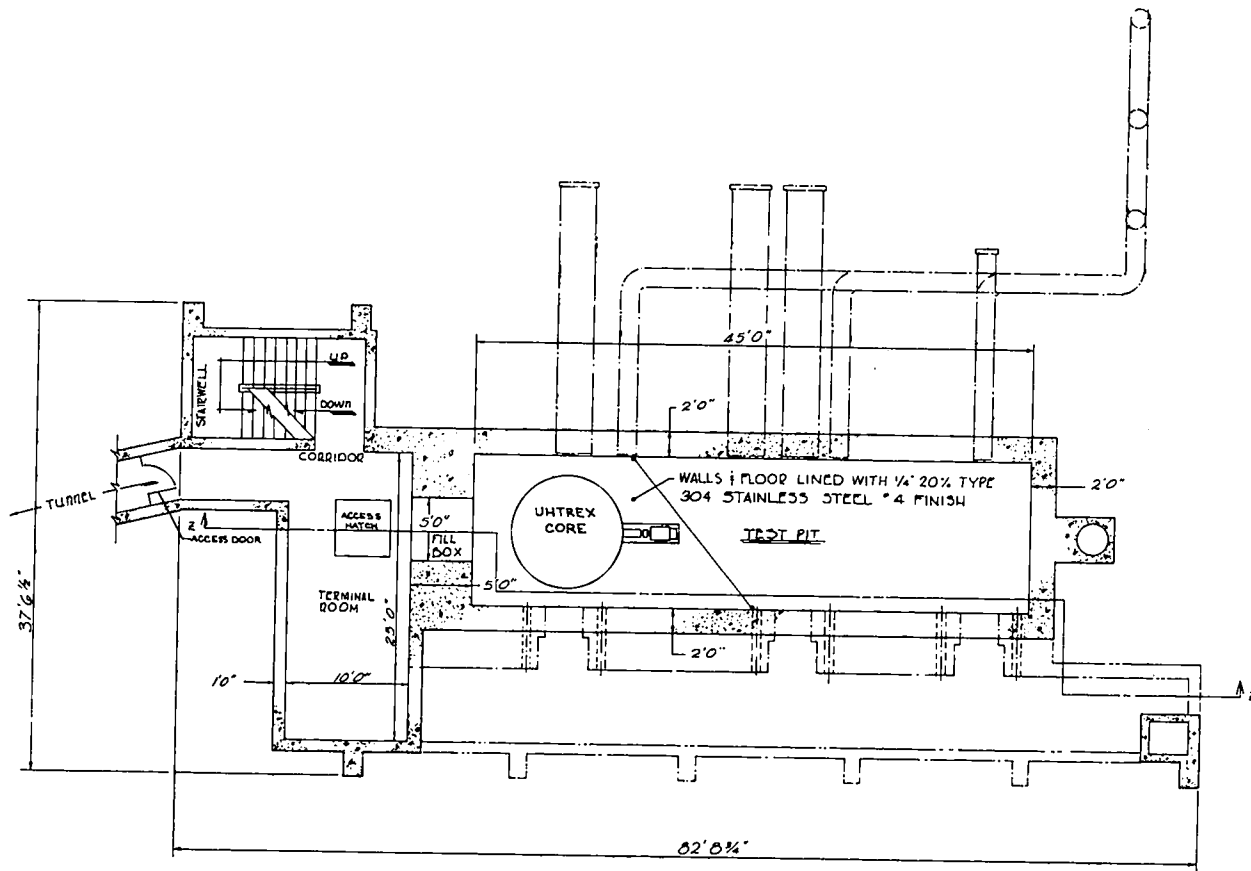


Fig. 3.2.1. Plan of pit building at grade level.



PLAN AT ELEVATION -15'-0"

Fig. 3.2.2. Plan of pit building at -15 ft level.

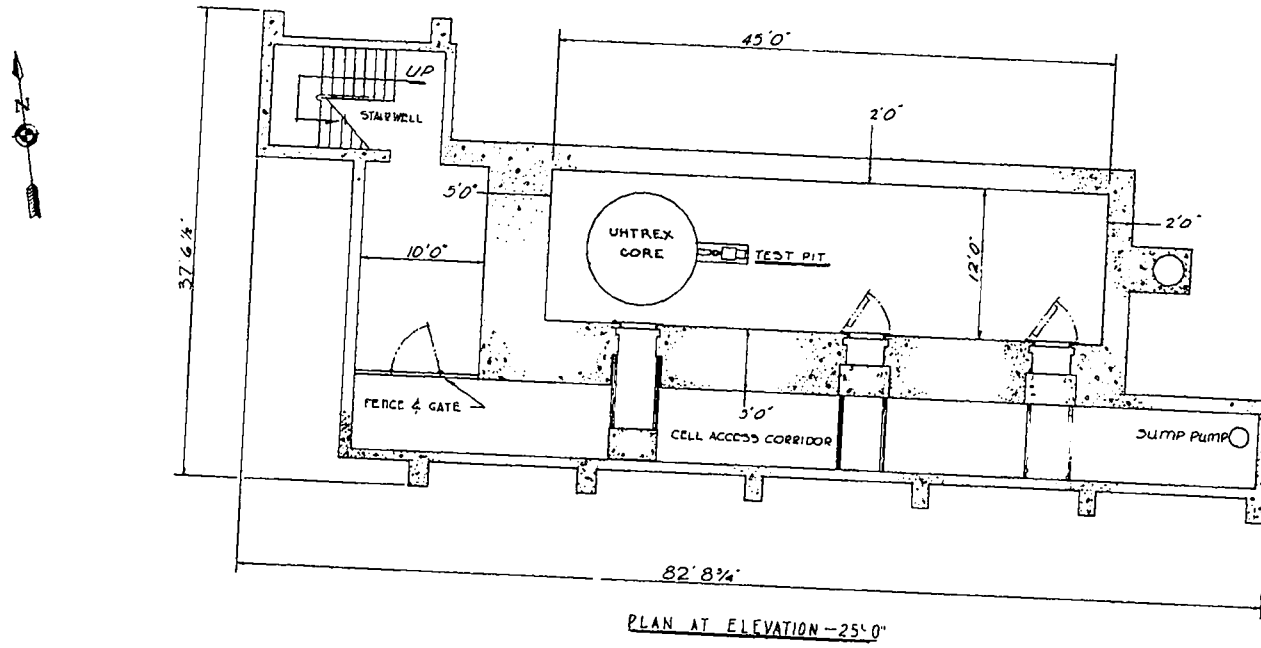


Fig. 3.2.3. Plan of pit building at -25 ft level.

3.2.1 Reactor Test Pit

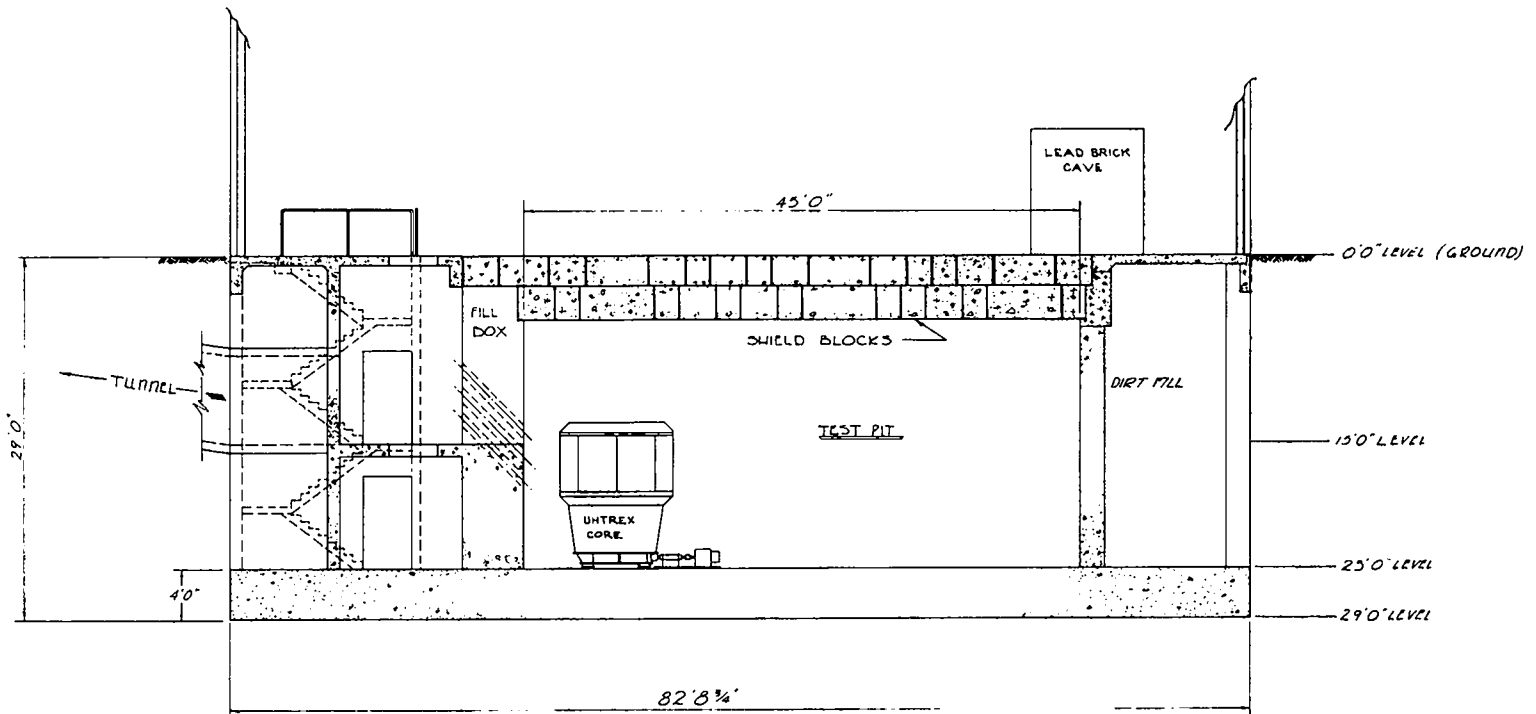
An elevation of the test pit can be seen in Fig. 3.2.1.1. The structure rests on a 4 ft thick slab of reinforced concrete. Exterior walls are 2 ft of concrete backed by earth and tuff rock. The internal walls that separate the pit from the terminal room and cell access corridor (see Fig. 3.2.2 and 3.2.3) are 5 ft of reinforced concrete. During critical experiments, the pit is covered with two layers of portable shield blocks, each 2-1/2 ft thick. The individual blocks, made of magnetite concrete, are sheathed in steel. The walls and floor of the pit are lined with 1/4 in., 20 percent type 304 stainless steel-clad plate, smoothly finished (see Fig. 3.2.1.2).

When the pit is covered, entry is made through one of the three doors off the cell access corridor at the -25 ft level. Each doorway is equipped with a hinged steel door that can be backed by a movable shield, 2-1/2 ft thick, made of concrete with Colemanite added.

At the west side of the pit, at the -15 ft level, a 5 ft wide fill box penetrates the wall. This opening is designed to permit the installation of a variety of auxiliary equipment pass-throughs to suit the core under test. During UCX, the box will be filled with shielding blocks. Details of this and other penetrations are given in Table 3.5.1.

3.2.2 High Bay

The high-bay portion of the pit building (TSL-29) is constructed of cemesto siding on a steel frame, with a sheet-metal and graveled roof. The structure is 37-1/2 ft wide, 82-1/2 ft long, and 32 ft high and has clear-glass windows in steel frames on the north and south sides. It is heated with gas-fired radiant panels and ventilated by two roof-top blowers. Access to the area is through a personnel door and a vehicle entrance at the east and west ends, and through an open stairwell from the tunnel at the -15 ft level. A 30-ton electrically



ELEVATION SECTION Z-Z

Fig. 3.2.1.1. Cross section of pit building.

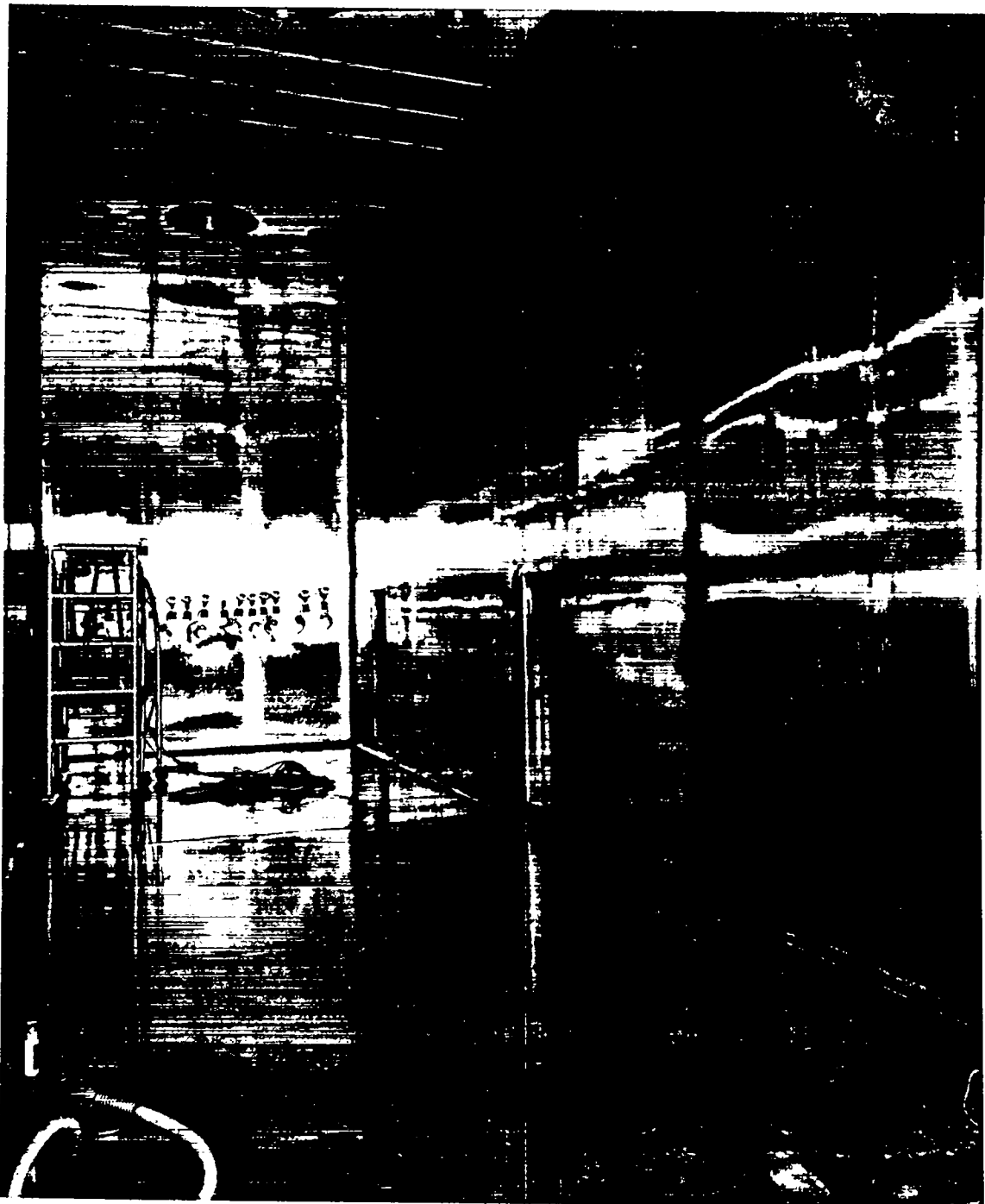


Fig. 3.2.1.2. Interior of reactor test pit.

powered bridge crane services the area within the high bay. The eastern 1/3 of the high bay area is temporarily occupied by a lead-brick cave used for studies of gamma spectra.

3.2.3 Terminal Room

On the -15 ft level, the tunnel enters the pit building at the terminal room, from which stairways lead up to the high bay or down to the access corridor. In the terminal room, wiring from the control room enters junction boxes or passes directly through penetrations into the test pit. A typical installation appears in Fig. 3.2.3.1. Much of the electrical power distribution equipment is located in the terminal room. The fill box occupies a portion of the 5 ft shield wall between this room and the pit. Two 4 ft x 4 ft hatches, one in the ceiling of the terminal room and one in the floor, provide access for lowering equipment with the crane from the high bay to either the -15 or -25 ft level.

3.2.4 Cell Access Room and Corridor

The cell access corridor at the -25 ft level runs the length of the pit, outside its south wall, from a room directly under the terminal room. The corridor is the route to the three doors into the pit. Normal entry to the -25 ft level is by the open stairway from the -15 ft level. A gate located at the south end of the access room prevents entry to the corridor during critical assembly operation. An escape trunk at the east end of the corridor provides an exit by ladder into the high bay area. The hatch can be opened only from the trunk side.

A sump tank, with duplex pump, in the east end of the corridor is available for collection and removal of any waste water which might find its way to the -25 ft level. The pump discharges to the contaminated sewer system.

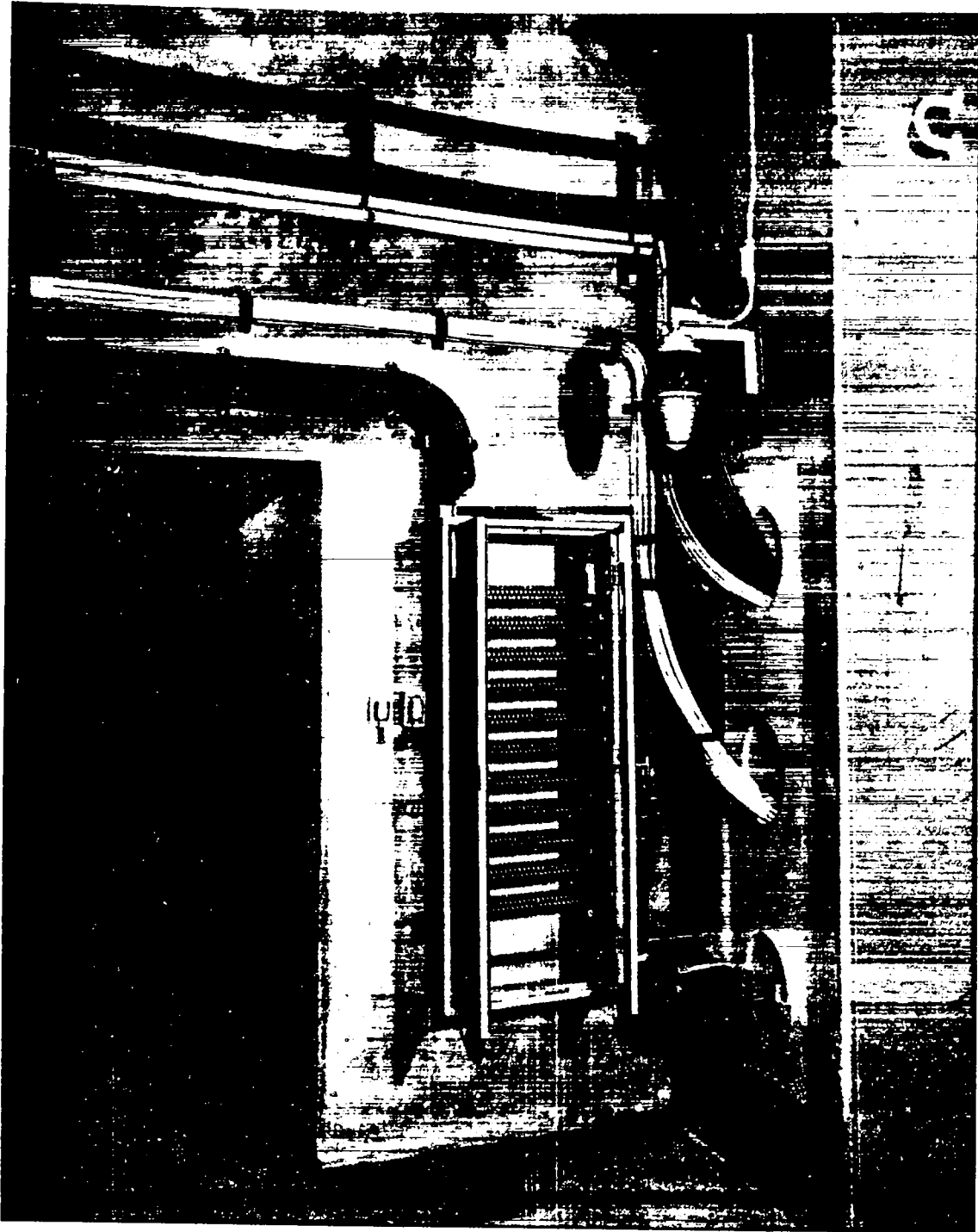


Fig. 3.2.3.1. Typical junction box and pass-through installations in terminal room.

3.3 Tunnel (TSL-35)

A concrete-lined tunnel, 80 ft long, 7 ft high, and 4 ft wide, connects the control room basement to the pit building terminal room. All wiring between the two buildings (TSL-26 and TSL-29) is routed along the tunnel. At the east end of the tunnel are a gasketed steel door and sealed cable penetrations.

3.4 Control Room Area (TSL-26)

The control room and its associated areas are located in the east end of Building TSL-26. A concrete block and reinforced-concrete structure, TSL-26 contains many shops, laboratories, and offices used by members of LASL's K-Division for the development of electronic, heat transfer, and fuel containment systems.

3.4.1 Control Room

The control room, 24 ft long x 21-1/2 ft wide, and 11 ft high, is located on the ground floor of TSL-26. It contains all the features usually found in a modern control room. The operating console is equipped with key-lock power switch, rod control switches and position readout, nuclear instrumentation readout and audible popper, a 48-point alarm annunciator panel, recorders, communications system, etc. The console is flanked by fourteen, standard, air-conditioned, instrument racks which can accommodate any array of electronic equipment. Building ventilation and utility monitoring, and health monitoring readout equipment are permanently installed in the racks.

3.4.2 Basement and Mezzanine

A large basement room is connected directly to the control room by a ladder and hatch, and is also accessible through a corridor and stairway. A mezzanine, at the south end directly under the control room,

supports installed junction boxes, relay cabinets, and thermocouple patch panels. The tunnel (TSL-35) enters the basement room at its southeast corner. At the north end of the basement are temporary offices used by K-Division personnel.

3.5 Shielding

The reactor test pit has 5 ft of ordinary concrete in its internal walls (between pit and controlled areas) and 2 ft of concrete for external walls, backed by earth and tuff rock. Five feet of magnetite concrete, in shield blocks, covers the pit. Shield penetrations are listed in Table 3.5.1, with the design features that maintain shield integrity. Calculations were made to check the adequacy of the existing shield for low power operation of UCX. The calculations are discussed below.

3.5.1 Neutron Shielding Calculations

Neutron fluxes to be expected at the outer surface of the core reflector region (radius 135 cm) were calculated with a two-dimensional diffusion code (CRAM). Results in flux-per-watt of power level are shown in Table 3.5.1.1. Estimates of dose rate beyond the shield are presented in Table 3.5.1.2. The dose rate estimates are based on concrete with 25 percent water retention and do not include allowances for penetration irregularities.

3.5.2 Gamma Shielding Calculations

Simplified calculations of volumetric gamma sources (prompt fission, core capture, and noncore captures) were based on neutron fluxes obtained from the CRAM code. Self-shielding was included by treating the core region and the graphite region outside the core as infinite slabs. The results of the flux calculations are presented in Table 3.5.1.1. Estimates of dose rates due to gamma radiation are presented in Table 3.5.1.2.

TABLE 3.5.1

LIST OF PENETRATIONS THROUGH SHIELD WALL

| <u>Penetration</u> | <u>Number</u> | <u>Size</u> | <u>Design Features</u> |
|--------------------|---------------|-------------|--|
| Access doors | 3 | 3' x 7' | Door shielded by 2-1/2 ft thick plug (concrete with Colemanite added) on wheels. Opening sealed by gasketed, dogged, liner door. |
| Ventilation | 3 | 16" diam | Pipe 15 ft below ground with 90° bend and long horizontal run before rising to surface at filter, fan, and stack pad. |
| Cable conduits | 18 | 8" diam | Conduits angled 45° upward into pit access corridor, three on each side of access doors. Unused conduits sealed by gasketed blanks. Used conduits sealed by gasketed plates with gas-tight connectors. All conduits filled with loose aggregate. |
| Fill box | 1 | 5' x 12' | Steel box sealed by plates on both pit and terminal room sides and filled completely with concrete blocks. |
| Cable conduits | 6 | 8" diam | Conduits angled 45° upward into terminal room, three on each side of fill box. Each conduit sealed at pit end by cable sealing boxes. All conduits filled with loose aggregate. |
| Heat dump piping | 6 | 36" diam | Corrugated pipe terminated by gasketed blanks 10' from south wall at point 12-15' underground. Pipe filled with sand. |

TABLE 3.5.1 (Continued)

| | | | |
|------------------|---|----------|--|
| Inspection holes | 3 | 35" diam | Steel-lined holes in shield block layers. Hole in each layer filled with stepped magnetite plug. |
| Inspection holes | 6 | 12" diam | Steel-lined holes in shield block layers. Hole in each layer filled with stepped magnetite plug. |

TABLE 3.5.1.1

SHIELD CALCULATION PARAMETERS AND RESULTS

| <u>Source</u> | <u>Flux at Reflector Outer Surface, per Watt of Reactor Power</u> | <u>Flux Equivalent to 1 mrem/h</u> | <u>Decade Length in Ordinary Concrete, Inches</u> | <u>Decade Length in Magnetite Concrete, Inches</u> |
|-----------------------------|---|--|---|--|
| Thermal Neutrons | $3.0 \times 10^5 \text{ n/cm}^2\text{-sec}$ | $250 \text{ n/cm}^2\text{-sec}$ | 6.4 | 2.2 |
| Above-Thermal Neutrons | $6.3 \times 10^4 \text{ n/cm}^2\text{-sec}$ | $10 \text{ n/cm}^2\text{-sec}$ | 12 | 8.7 |
| <u>Gamma</u> s E = 5 Mev | $1.2 \times 10^5 \frac{\text{photons}}{\text{cm}^2\text{-sec}}$ | $850 \text{ Mev/cm}^2\text{-sec}$ | 18 | 12.5 |

TABLE 3.5.1.2

DOSE RATES IN AREAS OUTSIDE TEST PIT

| <u>Area</u> | <u>Distance Core-to-Shield</u> | <u>Shield Thickness & Material</u> | <u>Dose Rates Per Watt (mrem/h)</u> | | |
|------------------------|------------------------------------|--|-------------------------------------|-----------------------------------|--------------------------|
| | | | <u>Thermal Neutrons</u> | <u>Above-Thermal Neutrons</u> | <u>Gamma (5 Mev)</u> |
| Pit Access Corridor | 19" | 60" Concrete | $<10^{-6}$ | 1.0×10^{-2} | 5.4×10^{-2} |
| Terminal Room | 36" | 60" Concrete | $<10^{-6}$ | 7.9×10^{-3} | 4.1×10^{-2} |
| High Bay Area | 110" | 60" Magnetite | $<10^{-6}$ | $<10^{-6}$ | $<10^{-4}$ |

3.5.3 Conclusions

The results of the shield investigation indicate the adequacy of existing shielding for UCX. Step-wise power rises, followed by neutron and gamma shield surveys, will be employed to assure below-tolerance dose rates in accessible areas outside the pit. If out-of-tolerance dose rates are found, the exclusion zones will be extended beyond the limits presently planned.

3.6 Utilities

3.6.1 Electrical Power

All conventional power (except some lighting) comes into the pit building from a 750 kva, 480 v, 3 ϕ transformer on the substation pad, TSL-32, just outside the southwest corner of TSL-29 (see Fig. 3.1.1). The power is fed to a distribution bus located inside the southwest corner of TSL-29 and from there to a 75 kva, 3 ϕ , 480 to 208/120 v transformer which feeds 3 ϕ , 208/120 v and 120 v outlets at the 0 and -15 ft levels in the pit building as well as in the tunnel and the mezzanine and control room in building TSL-26.

A 112.5 kva, 3 ϕ , 480 v to 208/120 v transformer, fed from switch gear in the southwest corner of the pit building and located in the cell access corridor (-25 ft level), feeds 208/120 v outlets in the reactor test pit and in the access corridor.

Instrument power also comes from the substation pad. However, a separate 25 kva transformer at the substation isolates instrument power from the regular building power. From this 25 kva transformer, power is fed to a 10 kva, 1 ϕ , 480 v to 120 v transformer located in the terminal room (-15 ft level) and to a 15 kva transformer located near the end of the tunnel in the basement of TSL-26. After passing through a multiple circuit breaker box (also in the terminal room), power from the 10 kva transformer supplies outlets in the reactor test pit, the access corridor,

terminal room, and the high bay. The 15 kva, 480 v to 120 v, 1 ϕ transformer feeds an instrument power breaker box which supplies the mezzanine area below the control room.

A large, quiet-ground cable (500 MCM) is installed throughout the power system to minimize ground loops which might affect low-level signals. The cable is welded to the stainless steel liner inside the reactor test pit and connected to the site ground (counter-poise) at the pit end. The other end is laid in the mezzanine cable trays.

Because the reactor test pit is a steel-lined room, the danger to personnel from electric shocks is greater than usual. To reduce the danger, power for portable electrical equipment in the pit is supplied through a 2.5 kva isolation transformer with ground-fault lights. The frames of the transformer and portable equipment are connected together and grounded.

3.6.2 Communications Systems

Intercom outlets are installed at twelve locations around the facility. Master stations, installed in five of the locations (control room, mezzanine, terminal room, cell access corridor, and in the test pit), can transmit to any other station.

Speakers connected to the central paging system at TA-35 are located at each level in the pit building and control room.

Telephone extensions are installed on each level of both buildings.

3.6.3 Fire Protection System

Heat sensitive fire detection devices are ceiling mounted on 15 ft centers, except in the test pit, throughout both the pit and control room buildings. An alarm from any one of these devices is indicated at the Los Alamos Fire Department's Central Station. Fire alarm boxes are located in the high bay area and in the control room basement area.

A fire hydrant is located within 75 ft of both buildings. Fire extinguishers of the CO₂ type are located on each level of both buildings.

3.6.4 Sump System

Floor drains in all below-grade areas of the pit building, except in the test pit, are routed to a 50 gal sump tank located at the east end of the access corridor. A duplex sump pump of 10 gpm capacity, at 30 ft head, discharges water from the tank to the LASL technical area contaminated sewer. The pump is started and stopped by float switch. The float also trips a high water level switch, at 2 ft depth, and actuates an alarm and light located at the southeast corner of the high bay.

3.7 Health Physics Instrumentation

Area monitors measure gamma radiation levels at the locations tabulated below:

TABLE 3.7.1

GAMMA MONITOR LOCATIONS

| <u>Location</u> | <u>No. of Monitors</u> | <u>Range (mr/hr)</u> |
|-------------------------------------|------------------------|-----------------------|
| Inside test pit, 10 ft from core | 2 | 1 - 10 ⁴ |
| Cell access corridor, south wall | 1 | 0.1 - 10 ³ |
| Terminal room, above tunnel door | 1 | 0.1 - 10 ³ |

Each of the gamma monitors has a local readout and alarm capability plus remote readout and alarm in the control room. Neutron, alpha, and air-borne particle activity surveys are made periodically with portable equipment.

A personnel monitor is located at the cell access corridor gate. Equipment for individual dosimetry and monitoring is provided, according to the LASL radiation safety policy.¹

Whenever the control panel is activated by the key switch, hazard warning lights are lit at five locations. The lights are mounted in the access corridor, in the terminal room, on the south wall inside the high bay, and outside the pit building at the east and west ends.

3.8 Ventilation

A schematic air flow diagram for the test pit building is presented in Fig. 3.8.1. The components of the ventilation system shown in the diagram are installed in the facility, and are available for use. However, the current experimental plans for UCX do not require use of the ventilation system.

3.8.1 Test Pit

Negative pressure in the pit can be maintained by one of two 2250 cfm blowers, located outside at the base of the stack, which draw air from the pit through absolute and charcoal filters and discharge through a stack 50 ft high. Air moves to the pit from the high bay through gaps around the shield blocks. Pressure drop across each of the two filter banks is measured at the filters and indicated in the control room. Each blower has a recirculating duct by which a portion of stack flow can be recirculated through the filter.

3.8.2 Access and High Bay Areas

Two, 3000 cfm, roof-top blowers can discharge air to atmosphere from the areas outside the pit, the stairwell forming the path from the lower regions. The -25 ft level is also ventilated by a 570 cfm fan, located outdoors at ground level, which draws air up the escape trunk.

¹ J. E. Dummer, Jr., and R. F. Barker, eds., "Radiation Monitoring Handbook," 3rd ed., LA-1385, November, 1958.

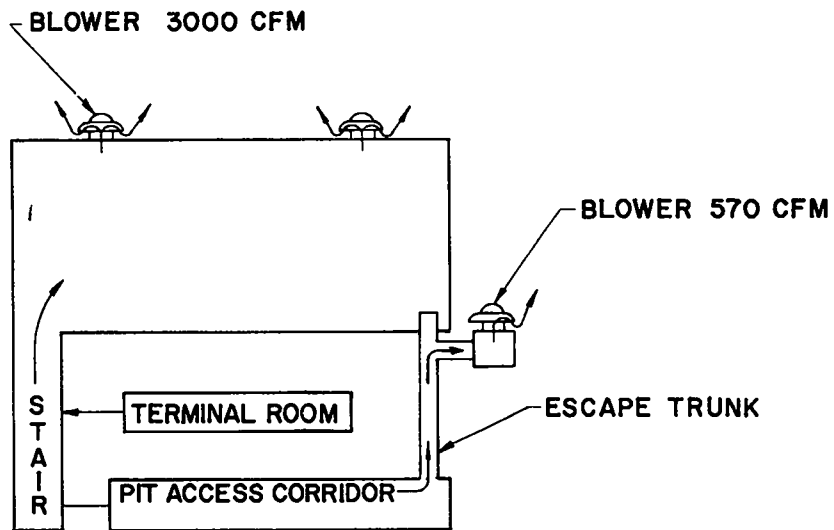
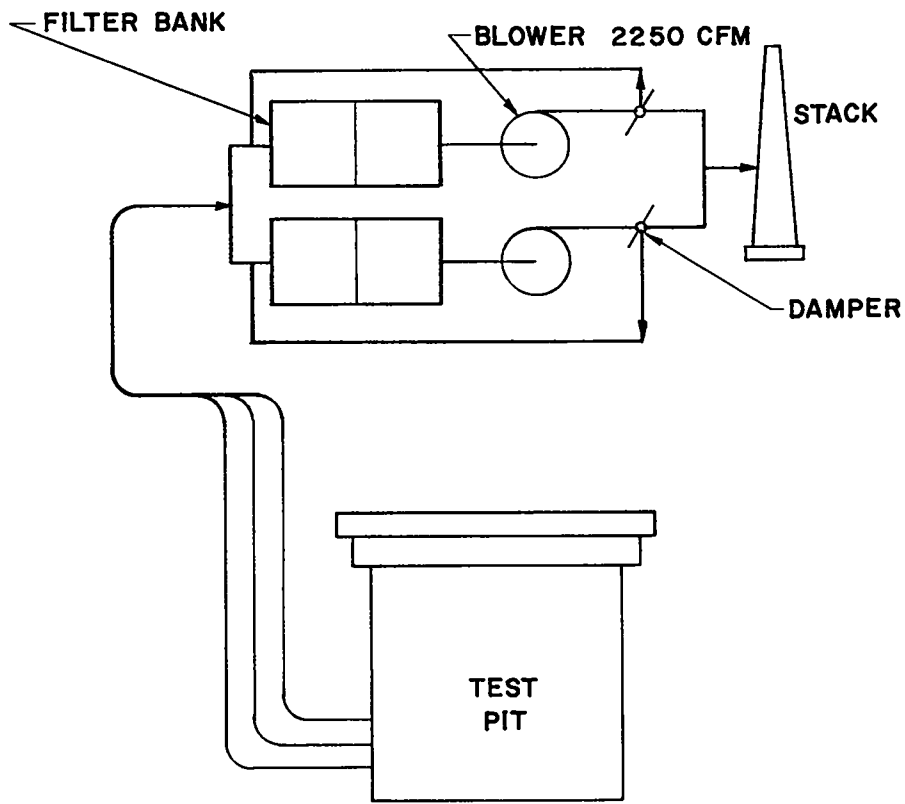


Fig. 3.8.1. Schematic diagram of pit building air flow

4. EXPERIMENT

4.1 Critical Assembly

The complete UHTREX reactor is described in detail in the UHTREX Hazard Report, LA-2689. Only the graphite core and the reflector, made of graphite and ungraphitized carbon, are used in UCX. A drawing of the UCX assembly, complete with control rod, startup source, and core rotation mechanisms, appears in Fig. 4.1.1. The components of the assembly are described below.

4.1.1 Core

The assembled graphite and carbon parts of the core and reflector are pictured in Figs. 4.1.1.1 and 4.1.1.2. Figure 4.1.1.1 shows a side view of the assembly resting on a support plate and drive mechanism designed for use in the UCX. Only the outer surfaces of the reflector and its supporting parts appear, penetrated by a slot, which is designed for the UHTREX fuel loader, and the thirteen holes through which fuel elements are loaded into the core. A top view of the assembly, Fig. 4.1.1.2, shows a central hole through the reflector top for the startup source, a circle of eight inner holes for the core plug control rods, and eight outer holes for the control rods in the rotating core.

Inside the reflector is the core, visible in Figs. 4.1.1.3 and 4.1.1.4. The core consists of a vertical, graphite cylinder, 70 in. o.d., 23 in. i.d., and 39 in. high, which serves as structure and moderator. It is mounted on a carbon support that rests on a large-

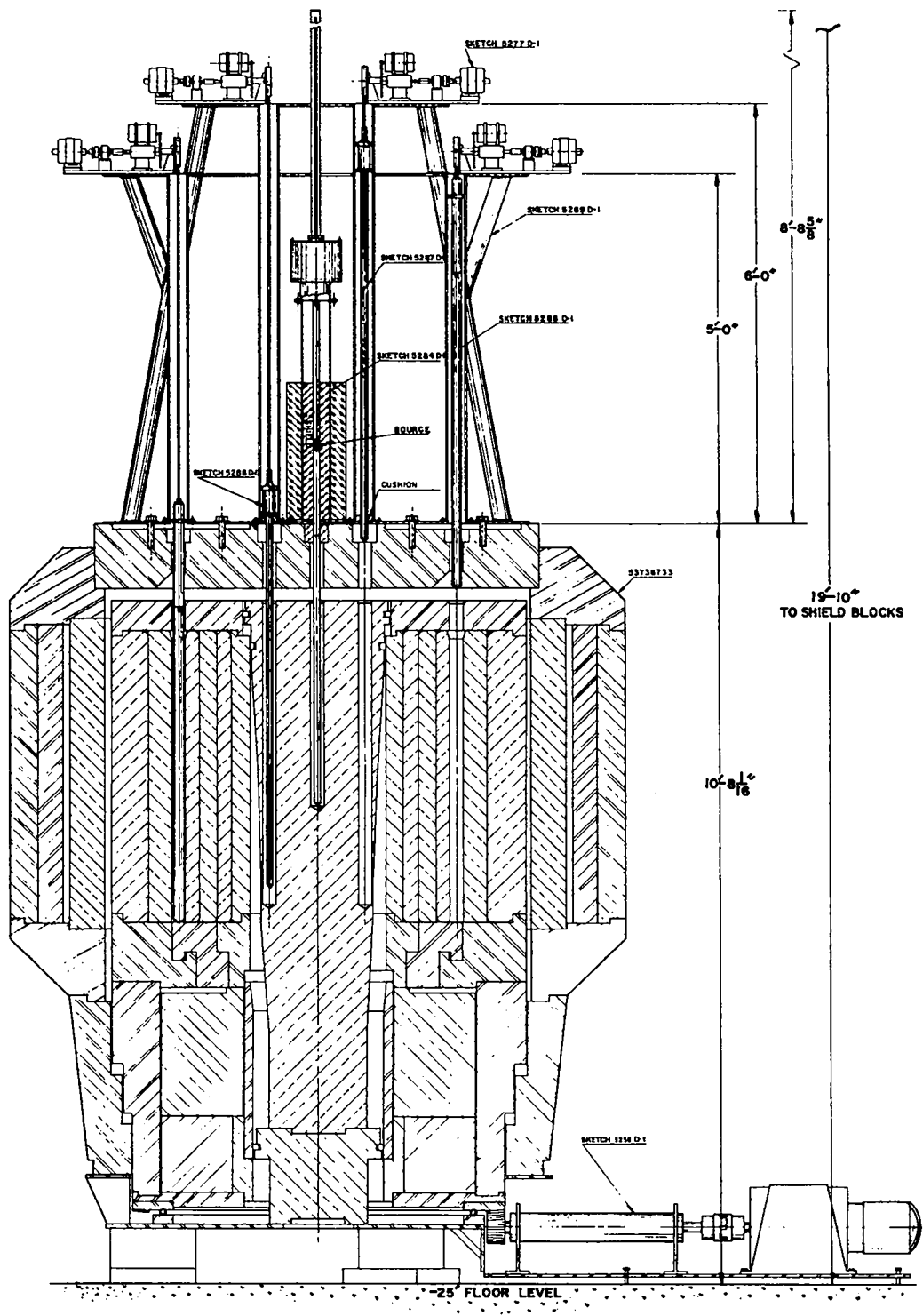


Fig. 4.1.1. UCX assembly, vertical section.



Fig. 4.1.1.1. UCX core and reflector assembly, side view.

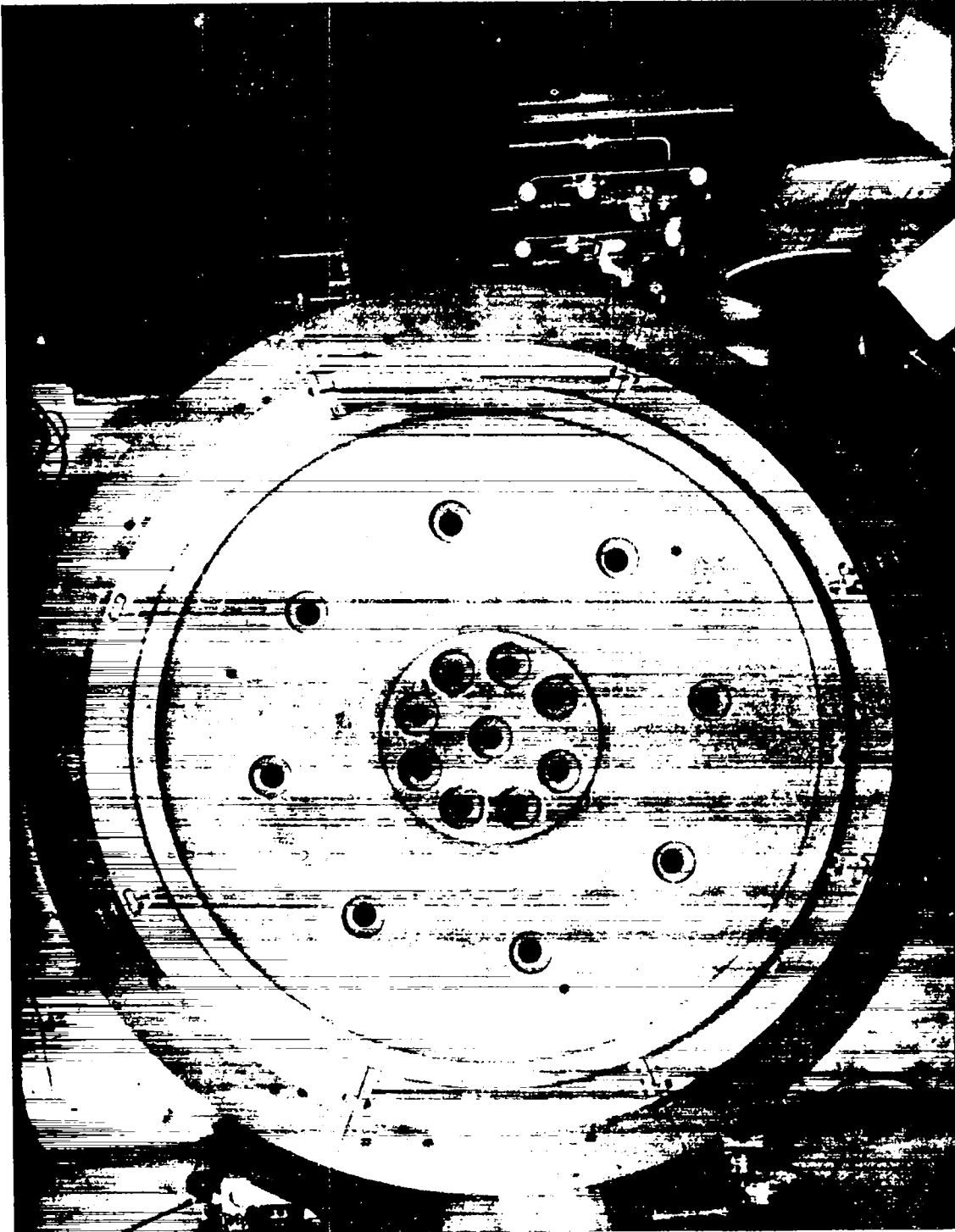


Fig. 4.1.1.2. UCX core and reflector assembly, top view.

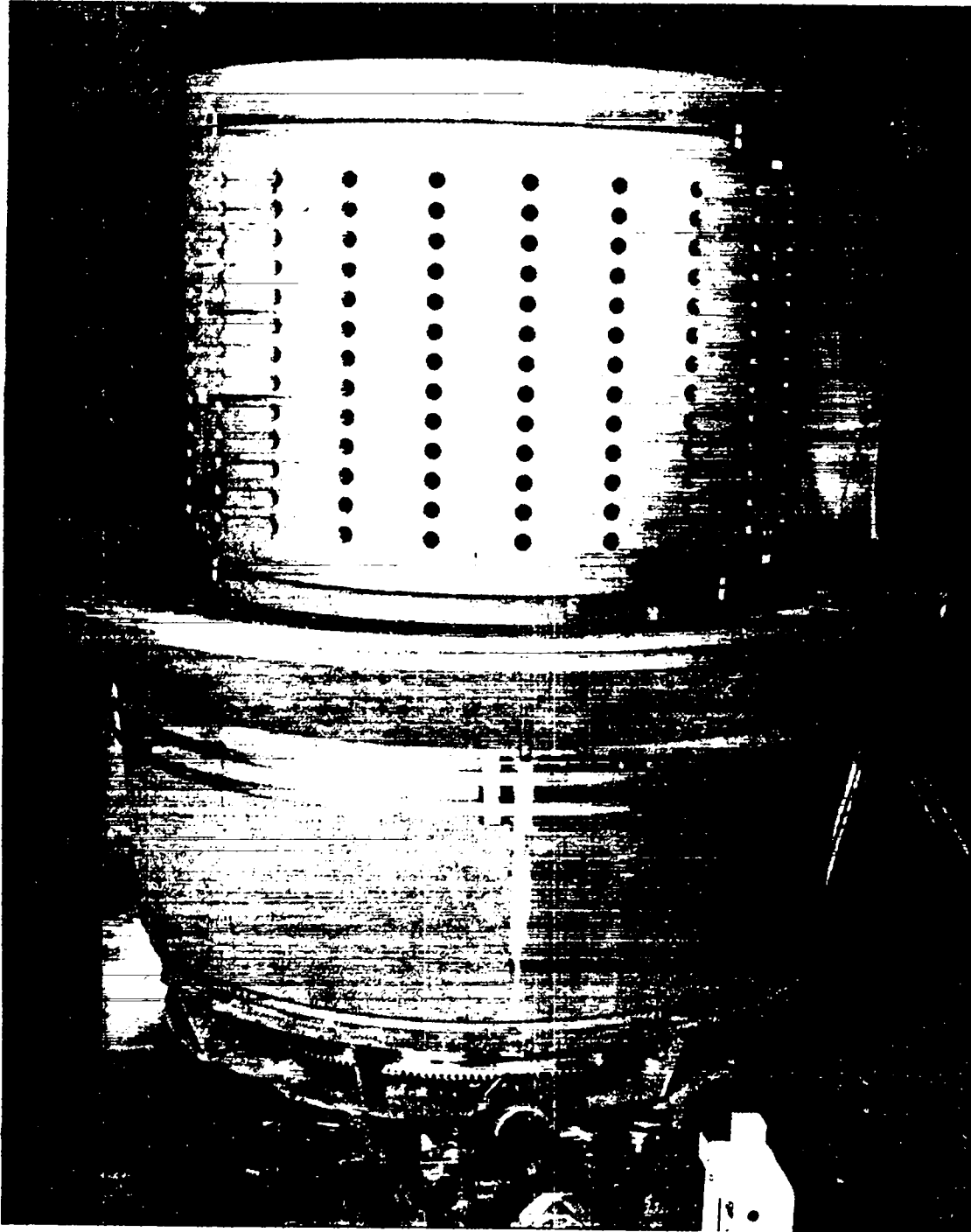


Fig. 4.1.1.3. UCX core assembly with central and top portions of reflector removed, side view.

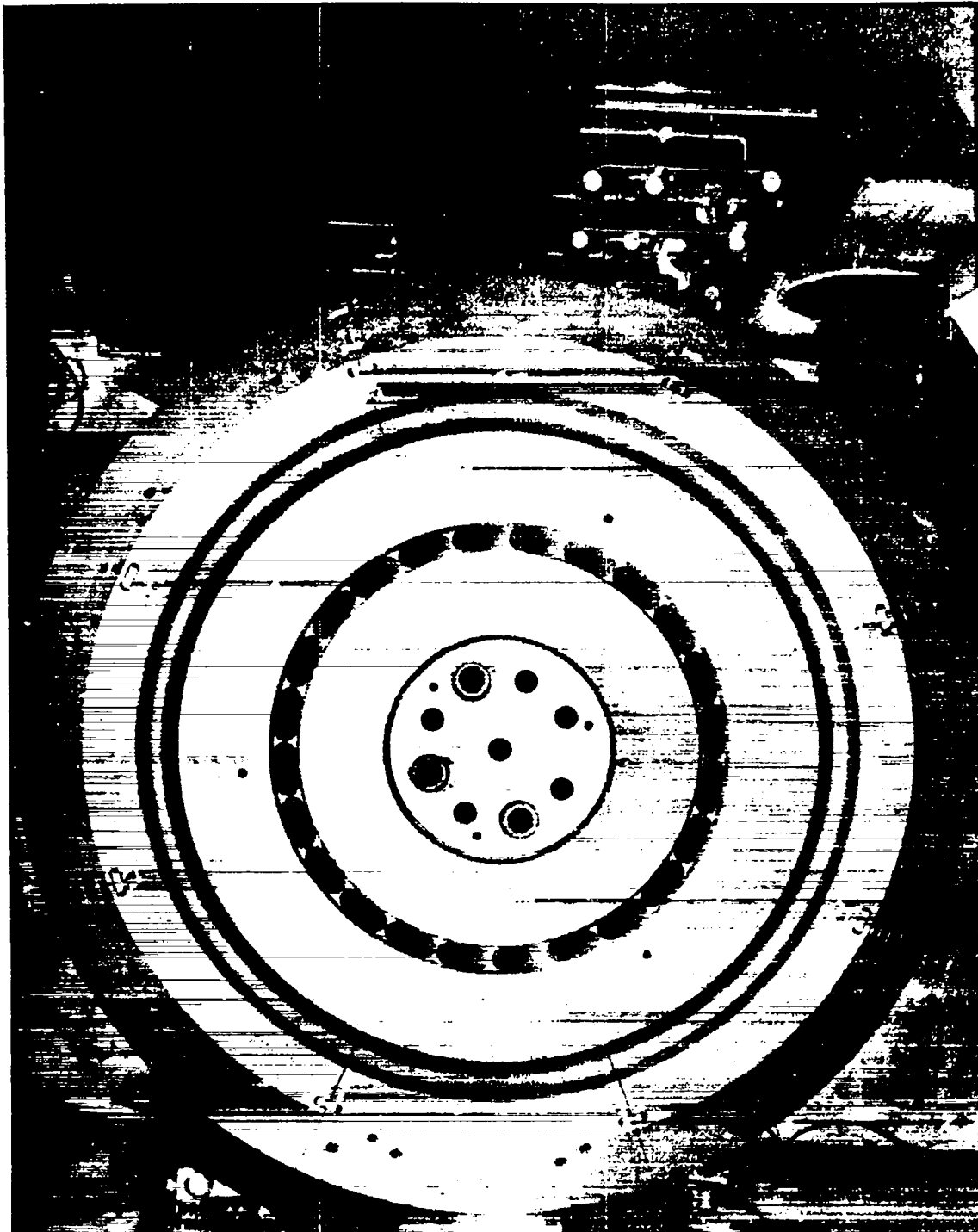


Fig. 4.1.1.4. UCX core assembly with central and top portions of reflector removed, top view.

diameter ball bearing with an integral gear, visible at the bottom of Fig. 4.1.1.3. Fuel channels are 1.1 in. diameter holes bored radially through the core wall at 15° intervals in thirteen planes. All of the core rotates around the vertical axis to accomplish fuel loading and unloading. For UCX a gear motor drives the core through a shaft geared to the integral bearing gear. To allow the insertion of all eight core control rods, at any of the 24 angular loading positions, the core has 24 vertical holes with flared tops.

A stationary graphite plug, visible in Fig. 4.1.1.4, fills the center of the hollow core. Within the plug are holes for the central startup source and eight control rods. In Fig. 4.1.1.4, three of the tubes that join the plug and the top of the reflector are placed in control rod holes.

4.1.2 Fuel Elements

Fuel elements are unclad, hollow, graphite cylinders, 1 in. o.d. x 0.5 in. i.d. x 5.5 in. long. Within the graphite matrix are highly enriched UC_2 particles, coated with pyrolytic carbon. Each PyC- UC_2 particle consists of a 105-149 micron diameter UC_2 core covered with 50 ± 5 microns of pyrocarbon coating.

In the loaded core, there are four fuel elements in each of 312 channels; the fully loaded reactor contains 1248 fuel elements. To provide the loading flexibility required for UHTREX, a total of 1560 elements will be prepared by CMB-Division at LASL. Fuel elements with five different loadings, ranging from 3.46 to 6.89 g of highly enriched uranium per element, are fabricated according to procedures that include rigorous quality control measures. At the start of fabrication, each stock piece, an extruded hollow cylinder made from carefully weighed charges of coated UC_2 particles, carbon, and binder, is embossed with a number that identifies the piece and its loading, expressed in $mg\ U/cm^3$. Later, each of the ten elements machined from this stock piece is

engraved with a serial number, based on the stock piece number, and the loading. When each element is complete, its loading is verified by a gamma count, calibrated against a chemical analysis of a sample of the stock from which the element was made. Finally, the elements are stored and transported in safe-geometry containers labeled with the identity of each element inside.

For UCX, one element at a time is loaded, according to an experimental plan, into the core, which is initially filled with unloaded fuel elements. Before each element is inserted, its identity is verified, by reading its engraved serial and loading numbers, and recorded on a fuel log. From the log, the fuel information is fed to a computer code that keeps track of the location of each element in the core and calculates the total core loading. As a visual aid, the experimenters place miniature color-coded dummy elements in a transparent mockup of the core to show the current status of loading.

To load a fuel element into the core, an experimenter inserts the element into the tube end of the loader tool, depicted in Fig. 4.1.2.1, inserts the tool into a loading hole, holds the tool against the insertion detent, and pushes the loader rod inward until the rod cap contacts the body of the tool. The motion of the rod pushes the element into the outermost position in the fuel channel and displaces the innermost element into the exit slot in the core plug. After the new element is in place, the experimenter withdraws the rod and removes the tool from the hole. If he should forget to remove the tool, the spring keeps the rod in its retracted position free of the core, and no damage is done when the core is rotated to a new loading position.

The displaced fuel element falls through the exit slot into a padded steel box that rests on the floor beneath the assembly. An experimenter then pulls out the box, which is mounted on wheels, and removes the element. Then he replaces the box within an alignment fixture mounted on the floor.

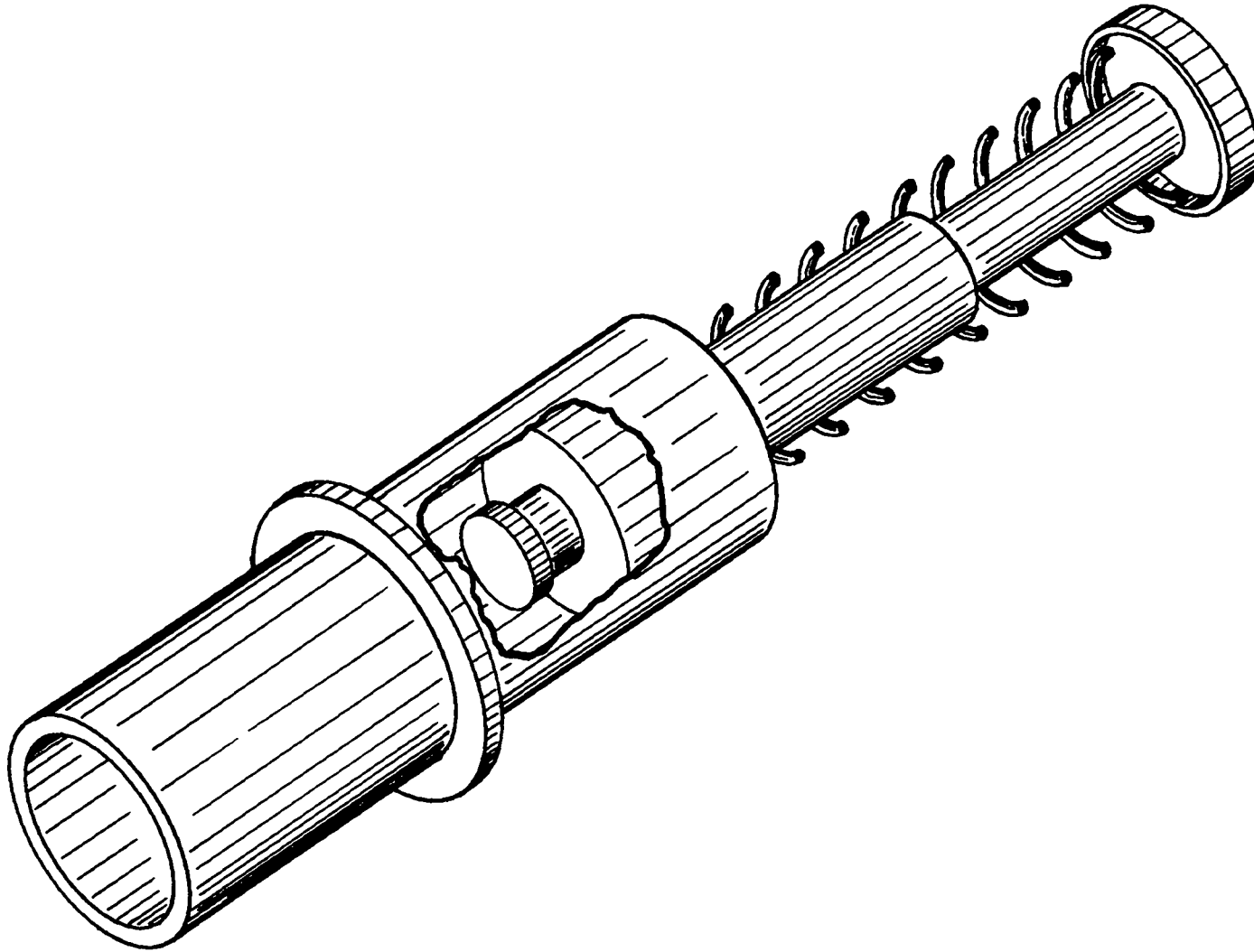


Fig. 4.1.2.1. UCX fuel loader tool.

Although UCX operates at such low power levels that no significant fission product inventory builds up in the fuel, each discharged element is checked with beta and gamma monitors before the element is removed from the discharge box, and all elements are handled in strict accordance with LASL radiation safety policy. The discharged elements are returned to their original containers for storage or transportation.

4.1.3 Control Rods

Instead of the actual UHTREX control rods, the UCX uses rods that are nearly identical in nuclear properties to the UHTREX rods but are contained in more economical structure materials that are adequate for the UCX environment. The active parts of the two sets of UCX control rods, eight in the central core plug and eight in the movable core, are made of the poison materials prescribed for the conditions in the UHTREX core at design temperatures.

For the central plug rods of UCX (see Fig. 4.1.3.1) aluminum tubes, 64 in. long x 1-1/4 in. o.d., contain stacks of B_4C compacts, hot-pressed to a density of 2.5 g/cc. The B_4C is not enriched in B^{10} . Active dimensions of each stack are 40 in. long, 7/8 in. o.d., and 0.41 in. i.d. Inside the close-fitting tube, each stack rests on and is covered with a neoprene disk and an aluminum disk. The void above the stack assembly is filled with low-density expanded plastic, compressed between the top aluminum disk and the tube cap. The restraint imposed by the plastic is sufficient to hold the B_4C stacks in place throughout the periods of acceleration and deceleration that occur after the rods are dropped.

Control rods for the movable core are made of type 304 L stainless steel, alloyed with 1 w/o B^{10} , machined to the dimensions of the UHTREX articulated control rods. For UCX, the articulated rods, each 39-1/2 in. long x 1-7/16 in. diameter are contained in a 54 in. long x 1-3/4 in. o.d. aluminum tube.

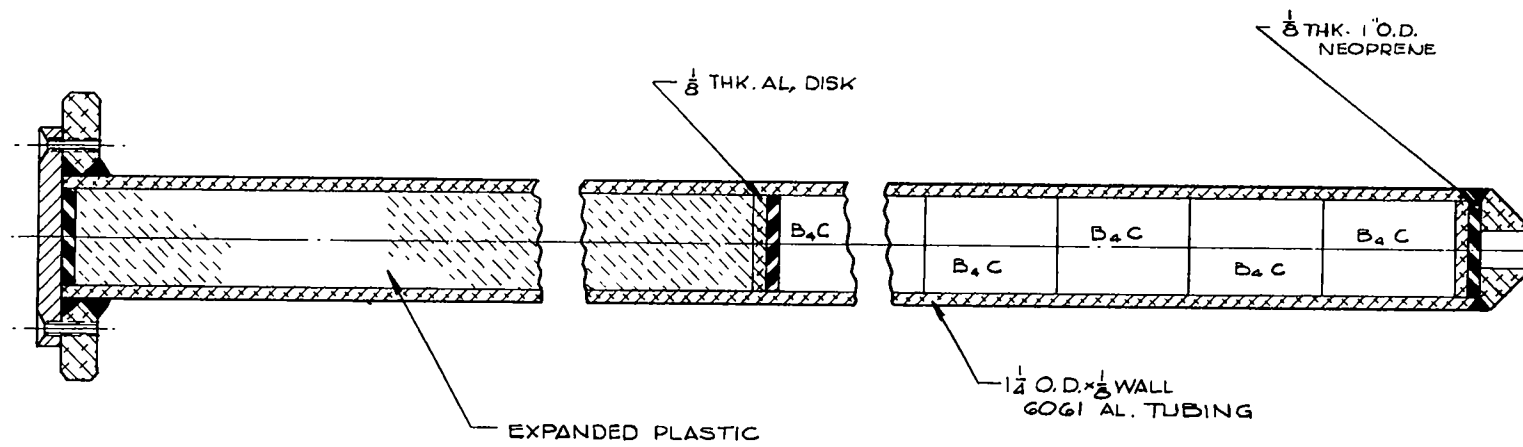


Fig. 4.1.3.1. UCX central plug control rod.

4.1.4 Control Rod Drives

The experiment will be conducted with five control rod drives. Three of the drives have scram capability and are of the type illustrated in Fig. 4.1.4.1. The electromagnet from which the rod hangs is fastened to a Teleflex cable that is vertically positioned by the pulley control box. Through the hollow center of the Teleflex cable, electrical wires deliver current to the magnet. The cable and control box act as a flexible rack and pinion.

The single-phase, capacitor-start, capacitor-run motor has an output shaft speed of 1725 r.p.m., reduced through a 1500 to 1 gear box. The Teleflex control box, running at 1.15 r.p.m., moves the cable and control rod at a linear velocity of 0.228 in./sec. For rod withdrawal, power is applied to the drive motor through a spring-loaded, normally-open, manual switch.

A scram is initiated through reliable, well-monitored circuits that act to interrupt current to the control rod drive magnets. Rods are released within 12 msec after a scram condition is reached and fall free into the reactor. Complete insertion occurs 0.6 sec after release. A shock absorber decelerates each rod at the bottom of its stroke.

Control rod position is indicated by a synchro system that drives a mechanical counter. Limit switches prevent over travel in the fully inserted and fully withdrawn positions. The drives are electrically interlocked so that only one rod can be withdrawn at a time. However, all rods may be inserted simultaneously.

The remaining two drives are identical to those described above except that electromagnets are not used. These two drives are designed to be moved. During the early part of the experiment they will be used to actuate plug rods. Later they will be used to actuate control rods that are located in the core. While a core control rod is attached to its drive unit, the core rotating mechanism is deenergized so that rotation cannot take place. When loading procedures require a movement of the core while the core rods are inserted, all core rods are detached from drives before the rotation starts.

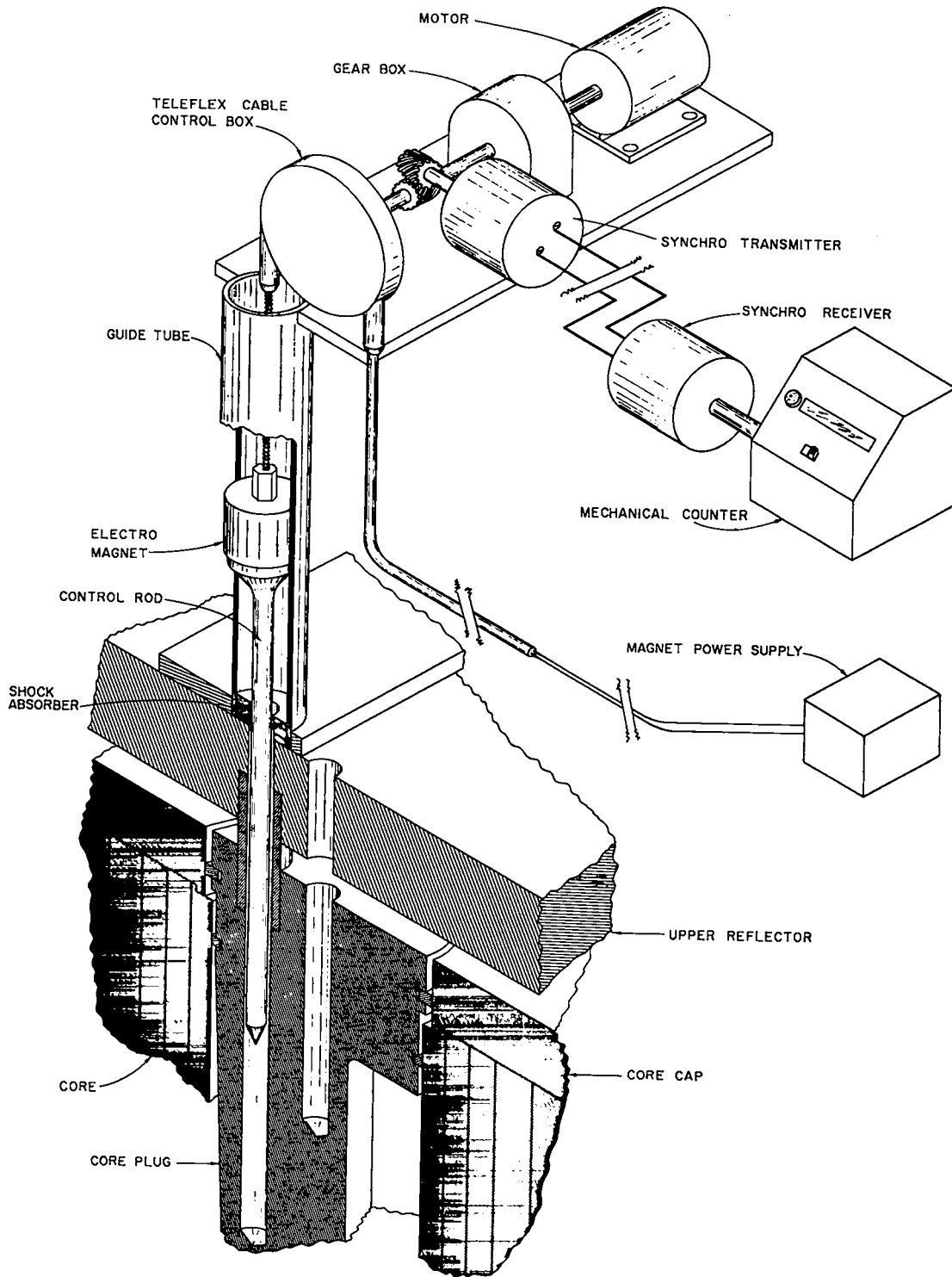


Fig. 4.1.4.1. UCX control rod drive with scram mechanism.

Core control rods that are not connected to a rod drive rest inside the rod holes in the core, clear of the reflector. The holes through the top of the reflector that correspond to the locations of the disconnected rods, are covered with plates bolted to the bottom of the control rod drive support structure (see Fig. 4.1.1).

4.1.5 Startup Source

A Pu-Be source, contained in a stainless steel capsule, delivers at least 10^6 neutrons/sec for use during core loading and reactor start-up. The source is positioned in the center of the core plug by a rack and pinion actuator. Limit switches indicate the source's position. It must be inserted into the center of the plug before control rods can be withdrawn. In the withdrawn position the source is located within a shield approximately 24 in. above the top of the core.

4.1.6 Nuclear Instrumentation

Nuclear data are collected by fourteen instrument channels discussed below. Figures 4.1.6.1 and 4.1.6.2 are block diagrams of the nuclear instrumentation.

Three pulse counter channels furnish neutron multiplication data during core loading. In addition these channels are used during routine approaches to critical when the assembly is operated with control rods.

Two linear electrometer channels serve as the primary data source while the assembly is critical. For the most part, determinations of incremental changes in reactivity are made by measuring stable reactor periods and applying the data to the inhour equation which yields reactivity.

Two Log N amplifiers are used primarily to derive reactor period. The period signal is displayed for operational convenience only and is not used for accurate data purposes. The Log N amplifiers also serve as wide dynamic range instruments to monitor flux levels.

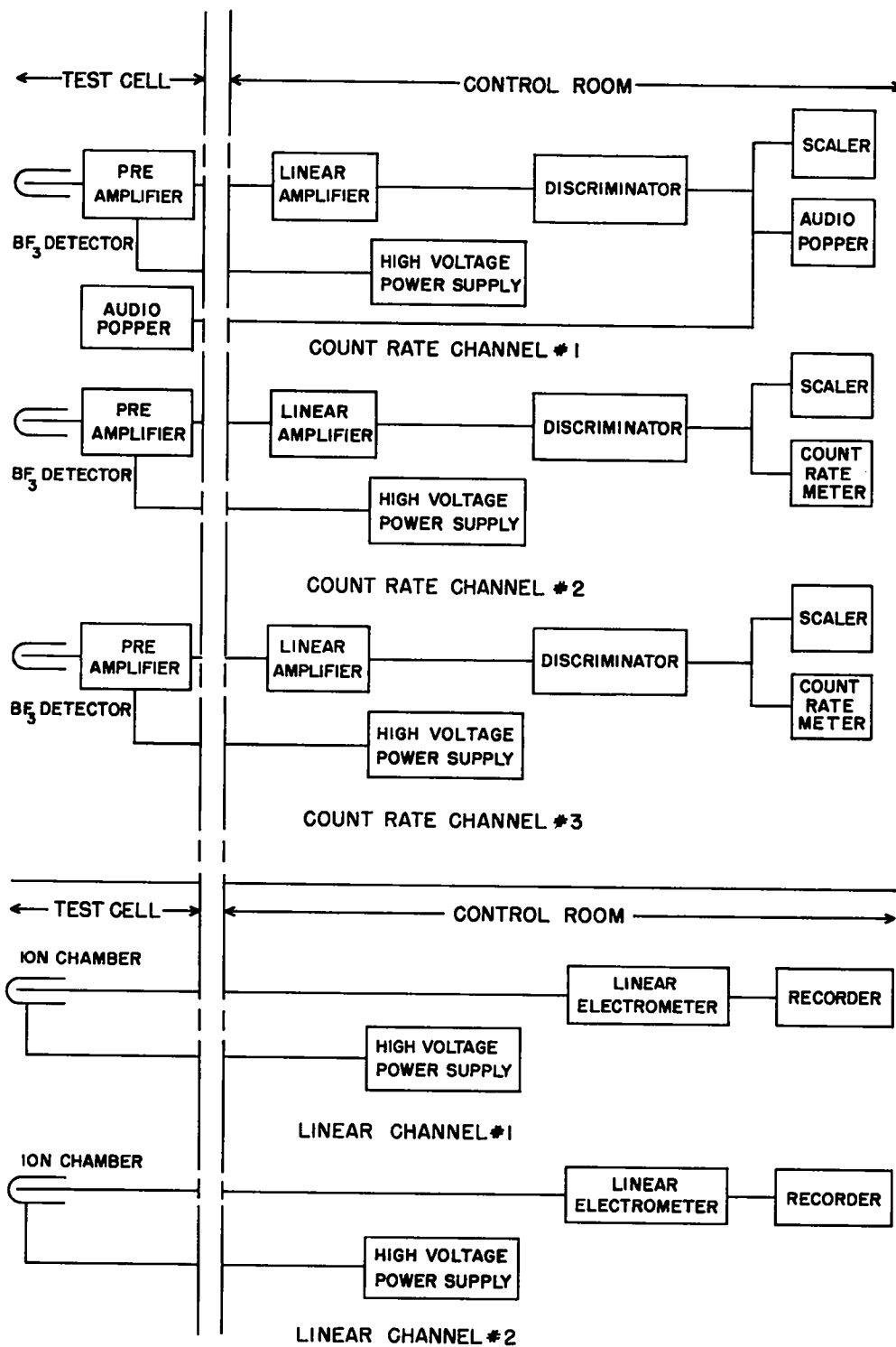


Fig. 4.1.6.1. UCX nuclear instrumentation channels, part 1.

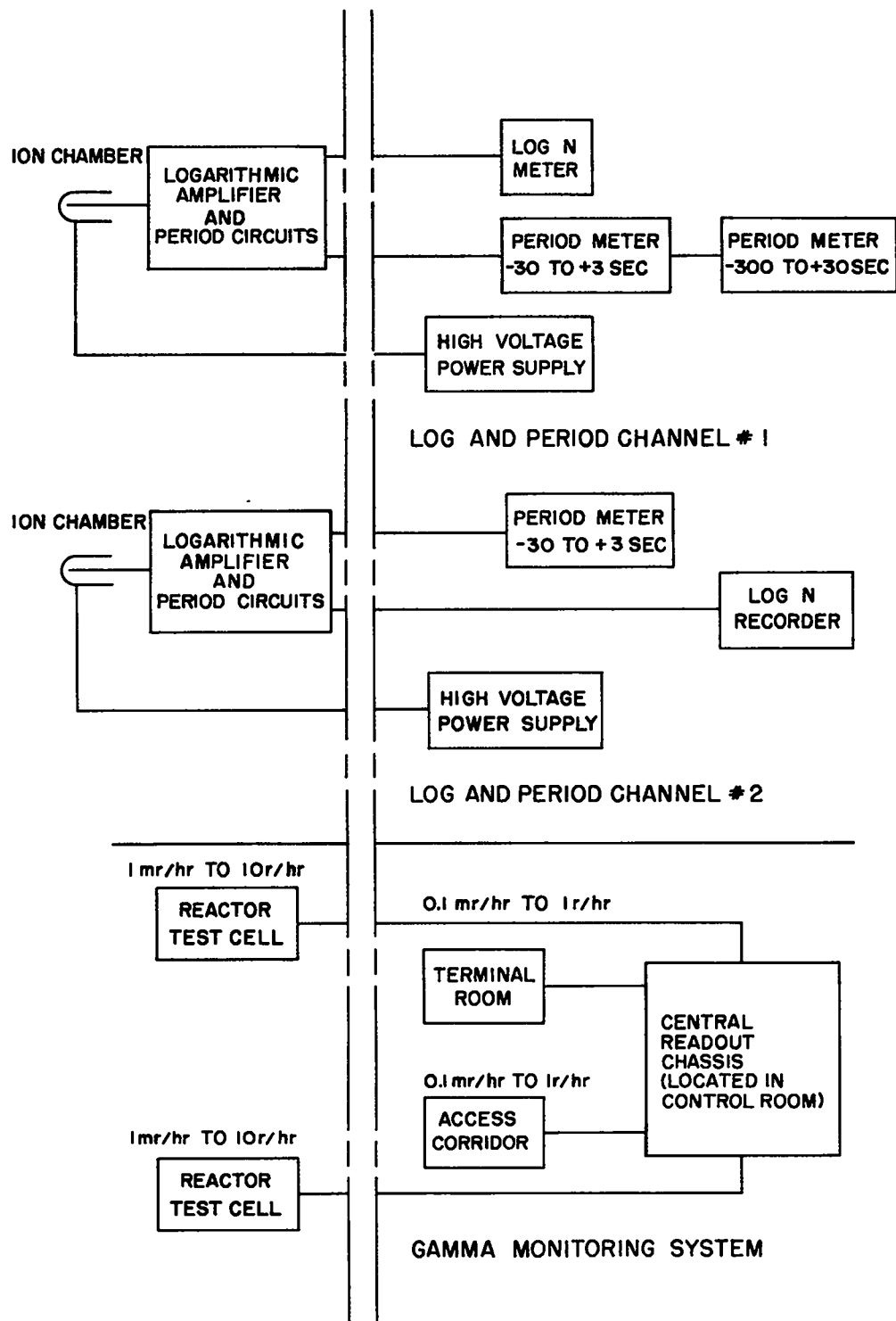


Fig. 4.1.6.2. UCX nuclear instrumentation channels, part 2.

Three independent safety channels, described in Appendix C, are used for automatic reactor shut down. They have one function: to provide automatic scram at a preset power level.

The gamma radiation monitoring system, described more fully in Sec. 3.7, consists of four remote stations and a central readout chassis. The latter is located in the control room. The range of each monitor is indicated in Fig. 4.1.6.2.

4.1.7 Non-nuclear Instrumentation

Six thermocouples are located in the core, plug, and reflector to measure temperatures during the temperature coefficient measurement.

4.2 Nuclear Operations

Performance of the UCX is planned in two phases. Phase I encompasses a series of experiments to be performed while an excess reactivity of less than $\$1$ is available in the reactor assembly. The objectives of the Phase I experiments are:

1. To determine the cold critical core loading,
2. To make a control rod calibration within the Phase I limits on excess reactivity,
3. To measure the power profile over the core,
4. To measure the reactor's temperature coefficient near the ambient temperature,
5. To investigate the effect of neutron source-detector geometry on measured neutron multiplication, and
6. To measure the effect on reactivity of voids or unloaded graphite in the place of fuel.

When Phase I is completed, calibration of the control rods is resumed in Phase II experiments.

4.2.1 Determination of Cold Critical Loading. (Phase I)

Because of the unique design of the UHTREX fuel loading system, fuel loading procedures are completely dissimilar from those used in other, more conventional, reactors. As was described earlier in Section 4.1.1, the core is a graphite cylinder with 312 radial fuel channels. When the reactor is fully loaded, each of the radial channels contains four fuel elements. The channels are loaded according to the prescription c , xc , x^2c , x^3c where the radially innermost element contains c grams of fuel, the next innermost element contains xc grams of fuel, etc.

The $x^n c$ prescription for fuel element loadings provides a means for obtaining approximately flat radial power distributions in the channels; and, in addition, provides the capability of maintaining a constant radial loading profile as the loading is increased. In design calculations which led to the fuel fabrication specifications in Table 4.2.1.1, the factor x was adjusted to the value 1.17. It is predicted that this value for the factor will provide satisfactory flattening of the radial power distribution in UHTREX at design operating conditions.

TABLE 4.2.1.1

UHTREX FUEL SPECIFICATIONS

| <u>Description</u> | <u>Number of Elements</u> | <u>Grams of Highly Enriched Uranium in Each Element</u> |
|--------------------|---------------------------|---|
| c | 312 | 3.46 |
| xc | 312 | 4.05 |
| x^2c | 312 | 4.74 |
| x^3c | 312 | 5.55 |
| x^4c | 312 | 6.49 |

By adding a fuel element containing x^4c grams of fuel to a channel containing initially the loadings c , xc , x^2c , x^3c , the innermost element

containing c grams is displaced into the exit slot in the core plug. The new channel loading then becomes x_c , x_c^2 , x_c^3 , x_c^4 , and each of the new fuel elements contains a factor of x more fuel than the corresponding elements in the preceding channel loading. This is basically the procedure for increasing fuel loadings in both UCX and UHTREX.

Specific loadings that will be achieved in the course of loading UCX are listed in Table 4.2.1.2. In loadings 5 and 7 all channels contain identical loadings. For the remaining loadings, two different channel prescriptions are listed. Alternate channels are loaded according to one prescription, and the remaining channels are loaded to the second prescription. Generally, in the approach to loading 1, and in the transition between any two consecutive loadings in Table 4.2.1.2, rotational symmetry is preserved.

The loadings in Table 4.2.1.2, which illustrate the UCX loading sequence, are specific cases for which k_{eff} values have been estimated. Criticality is expected in the neighborhood of loading 3, which contains about 4 kg of fuel. The tabulated k_{eff} for each loading is for the case with no rods inserted in the core. The rod worths of Tables 4.2.1.3 and 4.2.1.4 are used jointly with the loading k_{eff} 's to estimate net k_{eff} 's for loading and rod combinations.

A distinctive advantage of the UCX loading system is that the insertion of a single fuel element causes only a very small change in reactivity, of the order of 2 or 3¢ ($\sim 2 \times 10^{-4} \Delta k$). Furthermore, the manual insertion of an element requires times that are of the order of minutes. However, loading changes are performed only with the driven control rods inserted.

The rules of operation that govern manual loading procedures are summarized as follows:

TABLE 4.2.1.2

UCX CORE LOADINGS

| <u>Loading Numbers</u> | <u>Channel Loadings (Grams of Fuel per Element)</u> | <u>Total Mass (kgs)</u> | <u>k_{eff}</u> |
|------------------------|---|-----------------------------|------------------------|
| 1 | 3.46, 4.05, 4.74, 5.55 and 0 , 0 , 0 , 0 | 2.78 | 0.87 |
| 2 | 3.46, 4.05, 4.74, 5.55 and 0 , 0 , 0 , 3.46 | 3.32 | 0.94 |
| 3 | 3.46, 4.05, 4.74, 5.55 and 0 , 0 , 3.46, 4.05 | 3.95 | 1.01 |
| 4 | 3.46, 4.05, 4.74, 5.55 and 0 , 3.46, 4.05, 4.74 | 4.69 | 1.07 |
| 5 | 3.46, 4.05, 4.74, 5.55 | 5.55 | 1.13 |
| 6 | 3.46, 4.05, 4.74, 5.55 and 4.05, 4.74, 5.55, 6.49 | 6.03 | 1.16 |
| 7 | 4.05, 4.74, 5.55, 6.49 | 6.50 | 1.18 |

TABLE 4.2.1.3
WORTH OF RODS IN PLUG RING

| <u>Number of Rods</u> | <u>Worth (Δk)</u> | <u>Worth (\$)*</u> |
|-----------------------|--------------------------------------|--------------------|
| 1 | .029 | 4.5 |
| 2 | .057 | 8.9 |
| 3 | .079 | 12.3 |
| 4 | .097 | 15.2 |
| 5 | .111 | 17.3 |
| 6 | .123 | 19.2 |
| 7 | .133 | 20.8 |
| 8 | .141 | 22.0 |

TABLE 4.2.1.4
WORTH OF RODS IN CORE RING **

| <u>Number of Rods</u> | <u>Worth (Δk)</u> | <u>Worth (\$)*</u> |
|-----------------------|--------------------------------------|--------------------|
| 1 | .018 | 2.8 |
| 2 | .040 | 6.3 |
| 3 | .064 | 10.0 |
| 4 | .086 | 13.4 |
| 5 | .108 | 16.9 |
| 6 | .130 | 20.3 |
| 7 | .151 | 23.6 |
| 8 | .171 | 26.7 |

*The delayed neutron fraction, β , is assumed to be 0.0064.

**The core ring worths are reduced about 5 percent with eight rods inserted in the plug ring.

1. Key control procedures limit the use of the access gate and the control room console. The console and gate keys are affixed to a single key ring. Console power (consequently, rod drive power) is routed through a suitable switch on the access corridor gate so that, if the gate is opened, the rods will be inserted automatically in the same fashion as when the console key is turned off.
2. Counters are activated, and an audible count rate indication is maintained in the test pit and in the control room while loading changes are being performed.
3. Fuel is loaded only when the assembly is in its shutdown configuration. The shutdown configuration exists when all driven control rods are inserted. At least three driven control rods are available for shutting down the assembly during all operations.
4. The loaded mass does not exceed 90 percent of the estimated shutdown critical mass.
5. The loading sequence is governed by the prescriptions of Tables 4.2.1.1 and 4.2.1.2. The loading is performed in increments that are less than 10 percent of the estimated shutdown critical mass, and are less than one-half the difference between the estimated shutdown critical mass and the loaded mass. After each increment of fuel is added to the assembly, new observations of neutron levels are made with the driven rods both inserted and withdrawn. A reevaluation of the shutdown critical mass is then made before loading the next increment.
6. All operations are prescribed in written, approved experimental plans.

4.2.2 Initial Control Rod Calibration (Phase I)

After a loading is achieved that is near critical with all rods withdrawn, a partial calibration of the first rod in the plug ring is made.

Calibration of the rod requires a simultaneous evaluation of the worth of fuel element insertions. To perform the calibration, fuel is loaded in increments of about 10¢ ($6.4 \times 10^{-4} \Delta k$). After each incremental fuel loading, the new critical rod position is observed, and a period measurement made (by displacing the rod from its critical position) in order to determine the worths of the incremental rod and loading displacements.

After a reactivity of 90¢ ($5.8 \times 10^{-3} \Delta k$) is achieved with the first plug rod, further loading of fuel is discontinued until all other experiments, except for the remaining rod calibrations, are completed. Thus, the bulk of the experimental work is performed with less than \$1 in reactivity available. The consequences of the addition of 90¢ in reactivity at a maximum rate of rod withdrawal are described in Sec. 6.2.1.

4.2.3 Power Profile Measurement (Phase I)

The power profile over the core is determined from a gamma activity analysis of small diameter U_{235} wires which are inserted in the central fuel element coolant holes for irradiation. An absolute power calibration is obtained by radiochemical analysis of a number of fuel elements.

4.2.4 Measurement of Temperature Coefficient (Phase I)

An evaluation of the temperature coefficient is made by observing the displacement in the critical position of the calibrated rod when the temperature in UCX is raised the order of 10°C by hot air blown through the coolant channels.

4.2.5 Source Experiments (Phase I)

Solutions are sought in UCX to problems that concern the startup neutron source to be used in UHTREX. Because of the high temperatures in regions inside the 13 ft o.d. vessel, neutron detectors must be placed outside the vessel where there is a large attenuation in the neutron flux. Calculations show that a source placed at the center of the core assembly must emit at least 10^7 neutrons/sec to be detectable outside the vessel. Furthermore, the source must be protected by a suitable container against the high temperatures.

After a scram at high core temperatures, it might be desirable to restart UHTREX with only the inherent source of the reactor. Startup on the inherent source should be feasible. The principal inherent source, about 200 neutrons/sec, is produced by $C^{12}(\alpha, n)$ reactions which are induced by α particles from the decay of U^{234} . This source is large enough that statistical fluctuations in the neutron population should not cause appreciable uncertainty in the response to reactivity insertion rates of the order of $1\text{¢}/\text{sec}$ ($6.4 \times 10^{-5} \Delta k/\text{sec}$).

Studies of three general approaches to the source problem are planned for the UCX. First to be made is a survey of the attenuated fluxes and detector responses for the case of a strong central source (10^6 neutrons/sec). Next is a series of startups with the source withdrawn to successively greater distances from its central position. This set of experiments culminates in a startup on the inherent source alone. In the course of the planned experiments, a direct integral measurement of the magnitude of the inherent source is made, and the threshold multiplication levels at which detectors at various locations respond is determined. Finally, the possibility of using a strong source situated external to the UHTREX vessel is explored. The efficacy of a startup with an external source is impossible to predict with current computing facilities; consequently, this approach must be studied in an experiment.

4.2.6 Measurement of the Reactivity Effect of Unloaded Graphite and Void (Phase I)

For a series of reactivity effect experiments, fuel elements are replaced with unloaded graphite blanks and the change in reactivity is measured. The unloaded blanks are then removed and the effect of the resulting void is compared to the reactivity of loaded fuel elements.

4.2.7 Evaluation of Control-Rod System (Phase II)

After the completion of the Phase I experiments, the calibration of the control rod system is resumed in Phase II. As a first step, the calibration of the number one rod in the core plug is completed, according to the procedure discussed in Section 4.2.2. Then, the remainder of the rods are calibrated through the use of the original loading sequence described in Section 4.2.1. Each loading increment consists of an insertion of one element in each of the thirteen channels in one vertical row at one angular position. This increment gives a k increase of about 0.25 percent (39¢). The loading sequence of Table 4.2.1.2 is followed in selecting the successive loading increments.

In performing the measurements of the rod worths, it is essential to determine both the independent worths of the two rings of control rods, plug and core, and the amount of coupling between the two rings. To assess the degree of coupling, the worths of the first three rods in the core ring are determined with the plug ring inserted and with it withdrawn. No more than six of the plug rods are inserted while UCX is critical, because two of the plug rods are reserved for scram. The measurement of the independent worths of the two rings is made from separate observations of the critical configuration of each ring after each loading increment is inserted.

Estimates made from Tables 4.2.1.2, 4.2.1.3, and 4.2.1.4 show that a combination of six plug rods and three core rods holds down the maximum available loading of 6.5 kg. While this maximum loading is held constant, measurements on the core ring are completed by withdrawing plug rods to compensate for the addition of rods in the core ring.

In general, the rules governing loading procedures (see Sec. 4.2.1) apply to rod calibration procedures. An additional rule of operation that applies to rod manipulations is:

7. Rods are not withdrawn manually while fuel elements are in the core.

An auxiliary, remotely-controlled drive is used for withdrawing rods that are not normally connected to a drive.

An estimate of the consequences of withdrawing one complete rod at the maximum rate of 5¢/sec (3.2×10^{-4} Δk/sec), starting from delayed critical, is presented in Section 6.2.2.

5. SAFEGUARDS

5.1 Administration

A written description of all tests and experiments and of any modification that affects the nuclear characteristics of the UCX must be submitted to the UHTREX Planning Committee for review and approval. Experiments that involve operation of the critical assembly must also be submitted to the Division leader for his approval. The persons who propose an experiment prepare the written description. The UHTREX Planning Committee then appraises the soundness of the experiment and the experimental approach. If necessary, the committee is free to seek advice within the LASL before acting on a proposal. It is the UHTREX Planning Committee's responsibility to establish UCX operating procedures which are reviewed by the LASL Nuclear Criticality Safety Committee.

5.2 Initial Facility Checkout and Preoperational Tests

5.2.1 Control Rod Drives

Each control rod drive is tested to determine that it accurately positions and, under scram conditions, quickly releases a control rod. A number of tests are made to insure that all control rods which have scram capability are able to fall unrestricted into the core.

5.2.2 Source Actuator

The source drive is tested to determine that it properly moves the source from the center of the reactor to the source shield above the

core. Tests assure that the source is protected against mechanical misalignment or interference that might rupture the source container and contaminate the facility.

5.2.3 Nuclear Instrumentation

All nuclear instrumentation is tested to determine that it is dynamically stable and that it possesses reasonable drift characteristics. Tests determine the minimum signal levels at which useful data can be obtained and assure that electrical noise and interference do not significantly affect the collection of data or produce false scrams.

The ion chambers of the reactor safety system are tested to determine that they are linear. Chamber voltage required for linear operation is measured as a function of output current.

The count rate channels are calibrated in a fixed source-detector geometry. The calibration is repeated periodically so that consistent multiplication measurements can be made during fuel loading. Prior to the startup of each experiment, the response of the count rate channels is verified by exposing a neutron source at each detector.

5.3 Procedural Controls

5.3.1 Operating Limits

The core fuel loading does not exceed 90 percent of the shutdown critical mass. Shutdown is defined as the configuration with the driven control rods inserted. All rod withdrawals are performed under remote control. The maximum allowable rate of reactivity addition is 5¢/sec. At the beginning of any remote operation of the assembly, the two scram rods are withdrawn first. These two rods provide a minimum of \$3 of fast automatic scram.

5.3.2 Area Control

Although entry to the TA-35 security area is restricted to people on official business, the area immediately to the north of TSL-29 is a construction site where a 50-man crew is engaged in building the Fast Reactor Core Test Facility. Entry to the FRCTF site is open during normal daytime work hours and is restricted at other hours by locked gates controlled by the construction contractors. While the assembly is operating, warning lights are visible in the areas near TSL-29 and warning signs explain the significance of the lights. (Assembly operation is defined as any procedure during which the driven rods are withdrawn.) No excursion can occur that would result in a radiation hazard within the construction area.

Within the Test Facility, no entry is permitted to the test cell or to the cell access corridor during assembly operations. Prior to the start of any operation the test cell and access corridor are cleared of personnel, the gate at the west end of the corridor is locked, and the warning lights are turned on. The key to the access corridor gate remains at the control room console until the UCX is shut down.

5.3.3 Emergencies

Personnel in the Test Facility are warned of high radiation levels by both audio and visual alarms that trip when the gamma level exceeds pre-set values at any of the gamma monitoring stations. In areas occupied by personnel, the monitoring stations are set to alarm if the gamma levels exceed ten mr/h. If a radiation alarm is activated, personnel in the Reactor Test Facility report immediately to the control room.

5.3.4 Maintenance

Maintenance is defined as one-to-one replacement of defective components. Any change to a system that affects nuclear safety must be reviewed and approved by the UHTREX Safety Committee.

A log book is kept that describes the repairs and alterations. Electrical schematics and mechanical drawings are revised as needed to show all changes and modifications.

5.4 Interlocks

The written experimental plans that govern UCX include detailed procedures for the safe performance of all operations. To back up the procedural requirements of the plans, electrical interlocks act to interrupt operations that approach an unsafe condition and to prevent the resumption of operations before safe operating conditions are established.

Interlocks scram the assembly if any of the following conditions occur:

- a. Trip signal in one of the three safety channels.
- b. Power failure in the nuclear safety system.
- c. Open gate to access corridor.
- d. Execution of the manual scram.

Control rod withdrawal is prevented by interlocks until all of the following conditions are met:

- a. Gate to access corridor closed and locked.
- b. Manual and automatic scrams reset.
- c. Neutron source inserted in core.
- d. Reactor operation warning lights turned on.
- e. Console key turned on.

To aid personnel in establishing the state of the assembly, the existence of the following conditions is automatically indicated on an annunciator panel:

- a. Manual scram.
- b. Automatic scram.
- c. Open access gate.
- d. Neutron source not inserted in the core.
- e. Warning lights off.
- f. Core rotating mechanism energized.

6. HAZARDS

The characteristics of the UHTREX core make the UCX inherently safe. An excursion can occur only if a series of equipment failures happen concurrently and operating procedures are ignored. The consequences of a conceivable excursion are minor, and the effects are limited to the close vicinity of the reactor. Radical changes in reactivity can not be made by inadvertently adding or taking away fuel or moderator. Transients induced by the only means available, withdrawal of control rods, do no damage to the temperature-resistant fuel or core structure. Procedural restrictions prevent the exposure of operators to radiation during periods when large changes in reactivity are made.

6.1 Inherent Safety of the Core

Properties of the materials in the UCX core provide a considerable measure of protection against accidental excursions. At room temperature, the core ingredients lie thousands of degrees below their melting or vaporization points. Thus, such secondary effects as the explosive ejection of control rods, or other violent material relocations due to the rapid expansions of a material undergoing a change of state, are ruled out.

Temperature coefficients of reactivity of both the fuel and the bulk moderator are negative. The value of the fuel coefficient, α_f , is $-2.6 \times 10^{-5} \Delta k/^\circ\text{C}$ ($-0.41\text{c}/^\circ\text{C}$), and of the moderator coefficient, α_m , is $-2.3 \times 10^{-4} \Delta k/^\circ\text{C}$ ($-3.6\text{c}/^\circ\text{C}$). Because a large proportion of each fuel element is graphite, both the fuel and bulk moderator coefficients derive from neutron thermalization effects. As the temperature rises,

the thermal neutron spectrum hardens. The methods used in calculation of the temperature coefficients are discussed in Appendix D.

The effects of thermal expansions on temperature coefficients of reactivity are negligible. Therefore, inertial effects of expansions during fast transients have no influence on the shutdown mechanism. Although uncertainties exist both in the magnitude and sign of the doppler effect in highly enriched uranium, it can be stated with certainty that the doppler effect is negligible in UCX.

The core is totally reflected at all times by a thick graphite reflector. Therefore, it is impossible to significantly increase the number of neutrons returned to the core by adding material to the environment of the core. In particular, the effect of humans in the vicinity on neutron return is negligible.

Calculations also show that, since UCX is well-moderated, flooding the core with water decreases reactivity.

6.2 Reactivity Addition by Rod Withdrawal

Control rod drive speeds limit the maximum available reactivity addition rate to 5¢/sec. This rate is achieved only with the most valuable rod (number 1 plug rod) situated in its most valuable position (half withdrawn). At this reactivity addition rate, no significant energy release can occur if the scram circuits work. Furthermore, there is ample time for personnel to take corrective action, if, during rod withdrawal, a short period develops in the neutron power. Thus, a prolonged, complete lapse in the attention of the experimenters and failure of all scram circuits must occur simultaneously in order to produce a significant transient.

Although the above described combination of misadventures is improbable, an analysis of the consequences is performed to illustrate the response of the critical assembly to large transients. The method of analysis is described in detail in Appendix D. Two cases are

considered which cover the two phases of the experiment where (I) in the earlier phase of operations, only 90¢ reactivity is available and (II) in the later phase of operations, greater than 90¢ reactivity is available.

6.2.1 Case I: Available Reactivity is 90¢

In this hypothetical case, the reactor is critical with the first plug rod partially inserted to a position where complete withdrawal of the rod would introduce a positive reactivity of 90¢ ($\Delta k = 0.0058$). The rod is fully inserted initially, so that the reactor is at a multiplication of 40 or $\Delta k = -0.025$. The inherent source (200 neutrons/sec) is the only source available. A transient is created when the rod is withdrawn continuously to produce a constant ramp of +5¢/sec. Since it is assumed that the scram circuits fail to operate, the ramp continues until the rod is completely withdrawn.

The resultant transient is plotted in Fig. 6.2.1.1, and the pertinent excursion parameters are summarized in Table 6.2.1.1.

TABLE 6.2.1.1

CASE I EXCURSION PARAMETERS

| <u>Parameter</u> | <u>Value</u> |
|---|---------------------|
| Peak Power | 9 Mw |
| Energy Release | 175 Mw-sec |
| Peak Fuel Temperature | 407 °C |
| Moderator Temperature Rise | 11 °C |
| Time to Peak Power (from 1 watt) | 22 sec |
| Neutron Dose Outside 5' Concrete Shield | 40 mr |
| Gamma Dose Rate at Reactor: | |
| At Shutdown | 1×10^4 r/h |
| 1 Week After Shutdown | 0.8 r/h |
| Fuel Element Activity One Week | |
| After Shutdown | 0.8 mc |

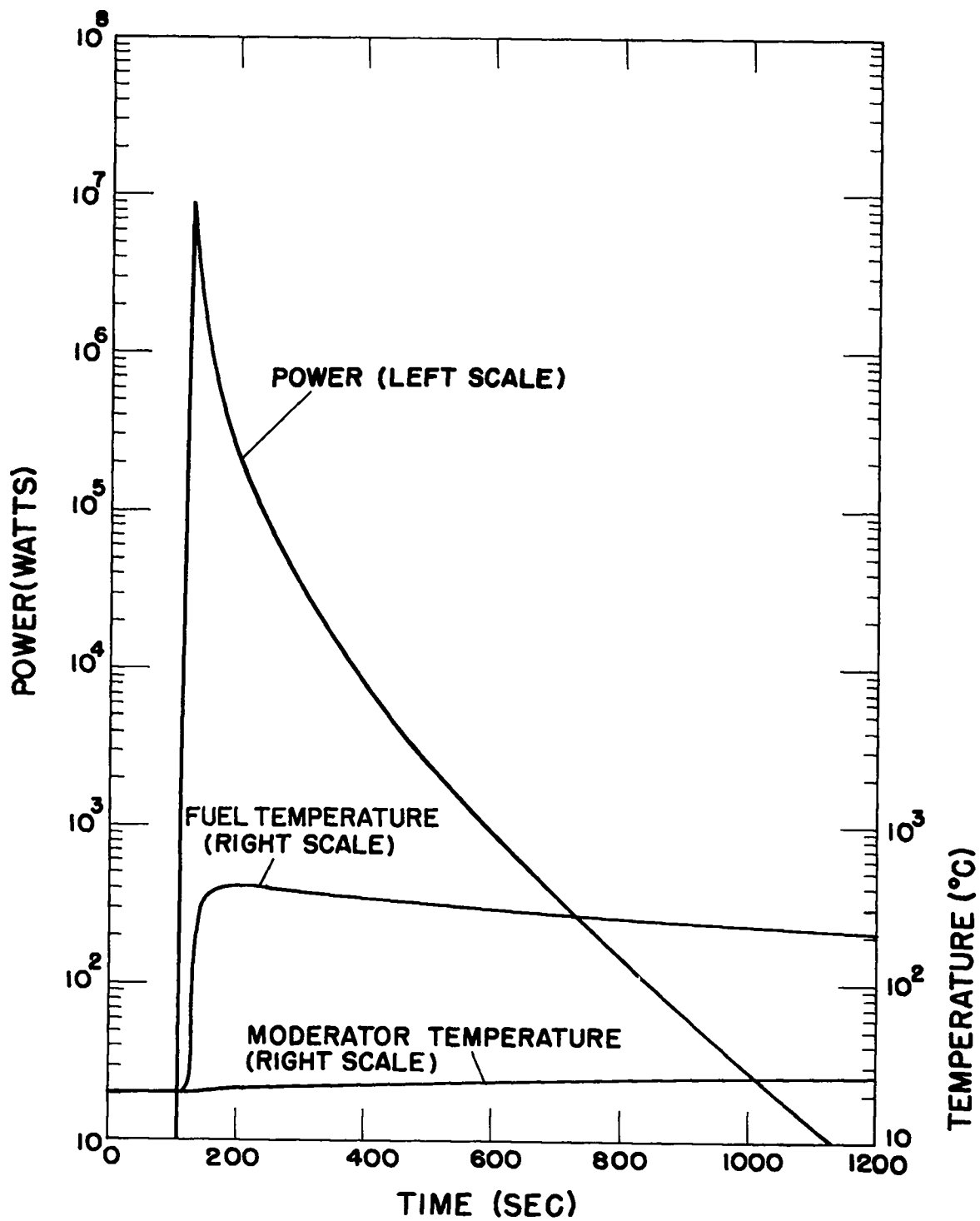


Fig. 6.2.1.1. Case I Transient.

The time required to withdraw the rod fully from its extreme down position is 96 seconds. (Actual rod withdrawals require 218 seconds. However, it is assumed conservatively that the rod, which has a total worth of 3.1 percent Δk (\$4.8), is withdrawn at the maximum reactivity insertion rate of 5¢/sec.) It is seen in Fig. 6.2.1.1 that the withdrawal is completed before sensible heating of the fuel begins. Virtually all of the 90¢ reactivity is compensated for initially by fuel heating; in fact, the maximum temperature rise in the fuel, 387°C, corresponds to a reactivity loss of \$1.57 ($\Delta k = -0.01$). Thus, this fuel temperature overshoot drives the reactor subcritical, which leads to the relatively slow fall in power after the initial sharp rise.

The most serious consequence of this excursion would be a restriction on reentry to the reactor pit for a few days. At the nearest point where personnel have access during reactor operations, the dose would be of the order of 40 mr. The temperature transient is far below that which would damage the fuel. Experiments on UCX-type graphite have shown that it may be heated to 1430°C and cooled in air without appreciable oxidation of the graphite.

6.2.2 Case II: Available Reactivity is Greater Than 90¢

In this hypothetical case the reactor is initially critical at 10^{-3} w power level, with the first plug rod fully inserted. Then, the rod is completely withdrawn at the constant rate of 5¢/sec. Scram circuits again fail. The resultant transient is plotted in Fig. 6.2.2.1, and the excursion parameters are listed in Table 6.2.2.1.

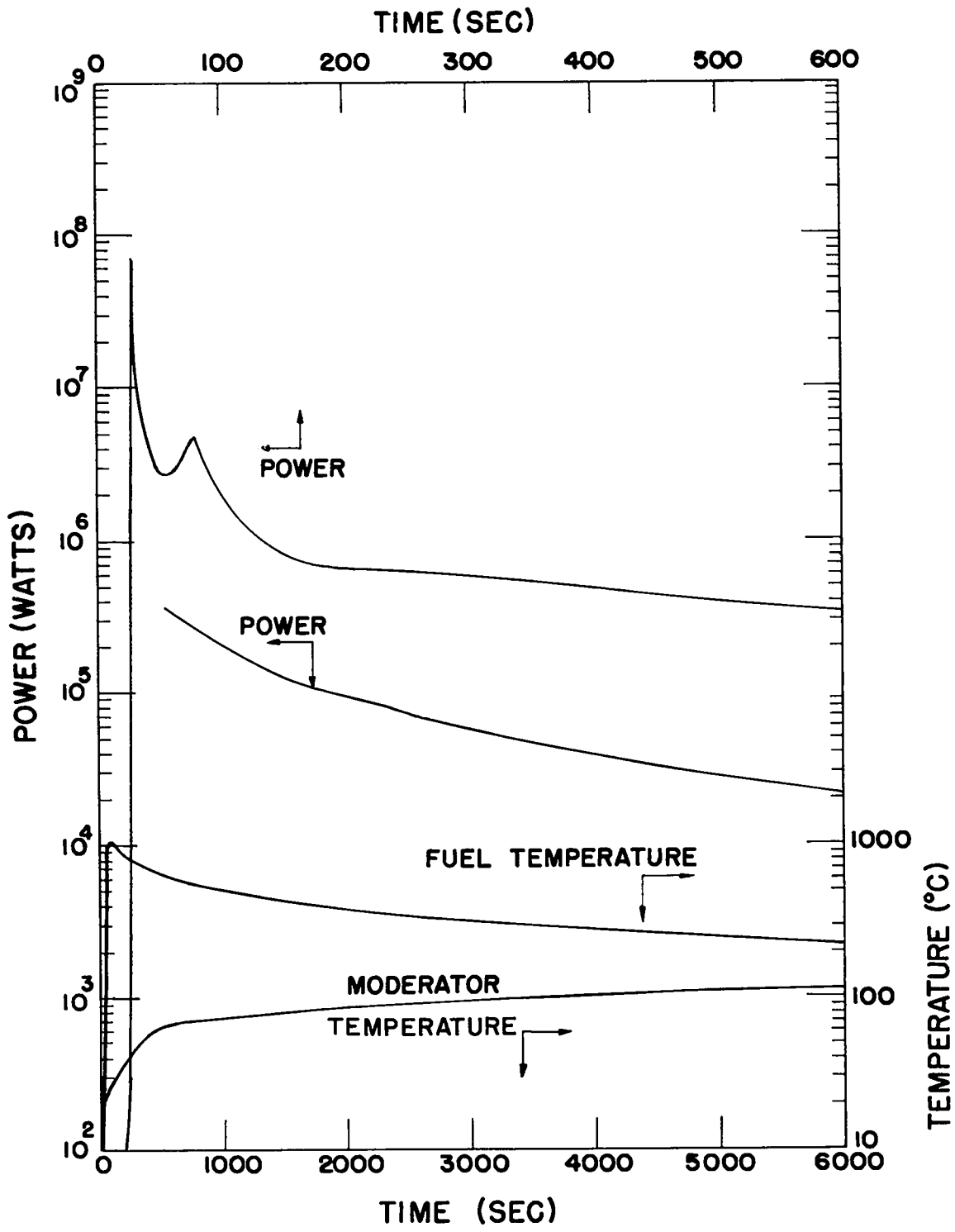


Fig. 6.2.2.1. Case II Transient.

TABLE 6.2.2.1

CASE II EXCURSION PARAMETERS

| <u>Parameter</u> | <u>Value</u> |
|---|---------------------|
| Peak Power | 74 Mw |
| Energy Release | 1070 Mw-sec* |
| Peak Fuel Temperature | 1020 °C |
| Moderator Temperature Rise | 90 °C |
| Time to Peak Power (from 1 watt) | 29 sec |
| Neutron Dose Outside 5' Concrete Shield | 0.3 r |
| Gamma Dose Rate at Reactor: | |
| At Shutdown | 9×10^4 r/h |
| 1 week after shutdown | 6 r/h |
| Fuel Element Activity | |
| 1 week after shutdown | 6 mc |

*Assumes shutdown after 6000 seconds.

In this transient, the first power peak is attained before the reactivity ramp is completed. Consequently, there is a secondary power peak, caused by the continued insertion of reactivity, which occurs at 80 seconds after the start of the ramp. Because of the greater reactivity insertion, this transient is more severe than the Case I transient. However, no damage would ensue, either to the facility or to personnel in the vicinity.

6.3 Reactivity Increases Through Mechanical Changes to the Assembly

It would be possible to increase reactivity if the top part of the reflector were pushed downward toward the core. Removing the void between the top of the reflector and the core increases $\Delta k/k$ by approximately 1 percent.

The top of the reflector is designed to support a uniform load of 133,000 pounds. The only credible mechanism for displacing the reflector downward is the dropping of a very heavy weight on top of the assembly. The shielding slabs that make up the roof of the test cell were designed to be removed with a crane. These slabs are very heavy and, if dropped, would undoubtedly crush the top of the reflector as well as alter the geometry of the assembly in other ways. Except for removing the void at the top of the core, the alteration would probably decrease the reactivity of the system.

To eliminate the possibility of dropping a slab on the critical assembly, the experiment is planned without a requirement to move the slabs. However, if an unforeseen situation should arise that would require the handling of slabs, fuel will be removed from the core prior to moving the slabs.

6.4 Reactivity Addition During Fuel Loading

Since only a single fuel element can be loaded at any given time, and since the addition of a single fuel element increases the reactivity by only 2 or 3¢, it would be difficult to achieve a significant power transient by loading fuel, even if all shutdown regulations were circumvented or ignored. Nevertheless, interlocks require that the source and the control rods be inserted whenever fuel loading operations are conducted. In addition, general regulations require that the effects of any fuel loading change be estimated before the change is initiated, be observed while the change is in progress, and be evaluated after the change has taken place.

APPENDIX A

METEOROLOGICAL DATA FOR LOS ALAMOS

TABLE A.1

AVERAGE WIND DIRECTION, LOS ALAMOS

PERCENT OF TIME

1953 - 1957

| SURFACE | Dir. | Jan. | Feb. | Mar. | Apr. | May | June | July | Aug. | Sep. | Oct. | Nov. | Dec. | Annual |
|----------------|------|------|------|------|------|------|------|------|------|------|------|------|------|--------|
| | S | 27.9 | 21.6 | 21.4 | 27.9 | 29.3 | 26.9 | 20.2 | 19.2 | 24.5 | 32.0 | 23.3 | 17.5 | 24.5 |
| | SW | 16.2 | 13.0 | 16.0 | 18.0 | 16.9 | 19.5 | 20.5 | 15.5 | 20.3 | 19.0 | 14.4 | 12.0 | 16.9 |
| | W | 13.8 | 16.0 | 21.3 | 21.7 | 18.5 | 22.3 | 16.6 | 21.0 | 20.2 | 15.2 | 15.3 | 15.5 | 18.7 |
| | NW | 7.7 | 10.5 | 10.9 | 8.2 | 7.4 | 7.3 | 8.5 | 8.5 | 7.3 | 7.2 | 9.4 | 10.6 | 6.9 |
| | N | 13.8 | 13.5 | 10.9 | 6.9 | 8.4 | 5.6 | 11.2 | 10.1 | 7.0 | 8.4 | 14.6 | 17.1 | 10.9 |
| | NE | 6.3 | 8.7 | 6.0 | 5.2 | 6.3 | 6.0 | 8.0 | 10.1 | 6.9 | 5.9 | 7.8 | 12.2 | 7.6 |
| | E | 7.7 | 8.9 | 8.5 | 7.8 | 8.9 | 7.6 | 9.2 | 10.1 | 8.2 | 6.6 | 8.7 | 7.4 | 8.6 |
| | SE | 6.6 | 7.8 | 5.0 | 4.3 | 4.3 | 4.8 | 5.8 | 5.5 | 5.6 | 5.7 | 6.5 | 7.8 | 5.9 |
| * UPPER AIR | Dir. | Jan. | Feb. | Mar. | Apr. | May | June | July | Aug. | Sep. | Oct. | Nov. | Dec. | Annual |
| | S | 11.9 | 5.7 | 10.7 | 13.8 | 18.4 | 30.6 | 17.7 | 26.7 | 22.8 | 20.9 | 8.9 | 6.5 | 16.2 |
| | SW | 18.6 | 16.1 | 22.1 | 14.4 | 25.0 | 20.2 | 24.2 | 20.0 | 18.8 | 22.1 | 15.0 | 15.9 | 19.4 |
| | W | 29.0 | 27.1 | 30.7 | 29.3 | 26.8 | 20.2 | 9.2 | 15.9 | 14.3 | 14.4 | 22.5 | 27.9 | 22.3 |
| | NW | 27.5 | 38.7 | 28.3 | 26.1 | 17.8 | 12.1 | 12.9 | 8.3 | 16.9 | 23.4 | 33.3 | 37.2 | 23.5 |
| | N | 8.6 | 9.2 | 4.5 | 8.6 | 7.0 | 8.9 | 6.9 | 10.1 | 8.6 | 8.6 | 15.0 | 9.4 | 8.8 |
| | NE | 1.1 | 0.3 | 0.0 | 2.8 | 0.0 | 3.2 | 4.6 | 3.7 | 4.0 | 1.6 | 2.7 | 0.3 | 2.0 |
| | E | 2.2 | 0.0 | 1.6 | 0.6 | 1.6 | 1.6 | 8.5 | 7.4 | 6.0 | 2.8 | 1.6 | 1.9 | 3.0 |
| | SE | 1.1 | 3.0 | 2.0 | 4.3 | 3.3 | 3.2 | 17.5 | 7.9 | 8.6 | 6.2 | 0.9 | 0.9 | 4.9 |

* About 1,000 ft above terrain; based on morning wind soundings at Albuquerque, data from three years of observation

TABLE A. 2
 AVERAGE SURFACE WIND SPEED, LOS ALAMOS
 PERCENT OF TIME
 1953 - 1957

| MPH | Jan. | Feb. | Mar. | Apr. | May | June | July | Aug. | Sep. | Oct. | Nov. | Dec. | Annual |
|-------|------|------|------|------|------|------|------|------|------|------|------|------|--------|
| 0 | 5.4 | 5.3 | 2.3 | 1.7 | 1.2 | 1.3 | 2.4 | 3.8 | 3.7 | 3.1 | 3.1 | 4.6 | 3.2 |
| 1-5 | 54.7 | 49.3 | 32.2 | 29.9 | 31.1 | 25.3 | 40.9 | 43.1 | 26.7 | 33.8 | 43.1 | 49.7 | 38.2 |
| 6-10 | 26.5 | 28.5 | 33.4 | 32.6 | 35.4 | 37.2 | 37.7 | 38.9 | 40.2 | 38.0 | 35.0 | 33.5 | 34.9 |
| 11-15 | 7.7 | 9.9 | 16.9 | 18.7 | 17.2 | 21.4 | 13.5 | 10.9 | 20.1 | 16.9 | 12.5 | 7.9 | 14.5 |
| 16-20 | 3.4 | 5.0 | 9.9 | 10.7 | 10.1 | 11.0 | 4.6 | 2.8 | 7.2 | 5.4 | 4.2 | 3.0 | 6.5 |
| 21-25 | 1.7 | 1.2 | 3.2 | 3.8 | 3.4 | 2.8 | 0.9 | 0.4 | 1.9 | 1.8 | 1.4 | 0.9 | 2.0 |
| 26-30 | 0.4 | 0.5 | 1.3 | 1.8 | 1.2 | 0.8 | 0 | <0.1 | 0.2 | 0.8 | 0.6 | 0.3 | 0.6 |
| 31-35 | 0.1 | 0.2 | 0.5 | 0.5 | 0.3 | 0.2 | 0 | 0 | <0.1 | <0.1 | <0.1 | <0.1 | 0.1 |
| 36-40 | <0.1 | <0.1 | 0.2 | 0.1 | 0 | 0 | 0 | 0 | 0 | <0.1 | 0 | <0.1 | <0.1 |
| 41-45 | <0.1 | <0.1 | <0.1 | <0.1 | 0 | 0 | 0 | 0 | 0 | 0 | 0 | 0 | <0.1 |
| 46-50 | 0 | 0 | <0.1 | 0 | <0.1 | 0 | 0 | 0 | 0 | 0 | 0 | 0 | <0.1 |
| 51-55 | 0 | 0 | 0 | 0 | 0 | 0 | 0 | 0 | 0 | 0 | 0 | 0 | 0 |
| 56-60 | 0 | 0 | 0 | 0 | 0 | 0 | 0 | 0 | 0 | 0 | 0 | <0.1 | <0.1 |

TABLE A. 3
PRECIPITATION, LOS ALAMOS
1952-1959

| | Jan. | Feb. | Mar. | Apr. | May | June | July | Aug. | Sep. | Oct. | Nov. | Dec. | Annual |
|--|------|------|------|------|------|------|------|-------|------|------|------|------|--------|
| Days of Precipitation | | | | | | | | | | | | | |
| Average | 9.9 | 10.1 | 11.8 | 10.9 | 14.6 | 10.9 | 20.0 | 20.9 | 8.9 | 7.7 | 7.0 | 7.3 | 155.2 |
| Maximum | 18.0 | 13.0 | 23.0 | 16.0 | 23.0 | 18.0 | 24.0 | 27.0 | 19.0 | 20.0 | 14.0 | 11.0 | |
| Minimum | 5.0 | 4.0 | 2.0 | 3.0 | 7.0 | 2.0 | 16.0 | 16.0 | 3.0 | 0.0 | 2.0 | 3.0 | |
| Days of Snow | | | | | | | | | | | | | |
| Average | 9.6 | 9.6 | 11.1 | 6.0 | 1.6 | 0.0 | 0.0 | 0.0 | 0.0 | 1.1 | 5.9 | 6.7 | 50.4 |
| Maximum | 16.0 | 13.0 | 23.0 | 12.0 | 4.0 | 0.0 | 0.0 | 0.0 | 0.0 | 3.0 | 10.0 | 11.0 | |
| Minimum | 5.0 | 4.0 | 2.0 | 0.0 | 0.0 | 0.0 | 0.0 | 0.0 | 0.0 | 0.0 | 2.0 | 3.0 | |
| Days of Thunderstorms | | | | | | | | | | | | | |
| Average | 0.0 | 0.3 | 0.1 | 1.8 | 7.6 | 7.4 | 16.3 | 17.9 | 4.9 | 2.6 | 0.4 | 0.0 | 60.6 |
| Maximum | 0.0 | 1.0 | 1.0 | 4.0 | 12.0 | 15.0 | 25.0 | 23.0 | 11.0 | 8.0 | 2.0 | 0.0 | |
| Minimum | 0.0 | 0.0 | 0.0 | 0.0 | 3.0 | 2.0 | 7.0 | 16.0 | 1.0 | 1.0 | 0.0 | 0.0 | |
| Precipitation (Since 1910) (inches) | | | | | | | | | | | | | |
| Average | 0.90 | 0.66 | 0.95 | 1.07 | 1.46 | 1.34 | 3.24 | 3.64 | 1.95 | 1.44 | 0.67 | 0.83 | 18.15 |
| Maximum | 6.57 | 2.44 | 3.27 | 4.64 | 4.47 | 5.57 | 7.98 | 11.18 | 5.79 | 6.77 | 3.30 | 2.27 | 30.34 |
| Minimum | 0.0 | Tr | Tr | 0.0 | 0.0 | 0.0 | 0.72 | 0.51 | Tr | 0.0 | 0.0 | 0.05 | 6.80 |
| Snowfall (1952-1959) (inches) | | | | | | | | | | | | | |
| Average | 9.0 | 8.7 | 11.1 | 4.4 | 0.1 | 0.0 | 0.0 | 0.0 | 0.0 | 0.3 | 4.8 | 7.7 | 46.1 |
| Maximum | 18.8 | 18.0 | 35.5 | 33.6 | 4.0 | 0.0 | 0.0 | 0.0 | 0.0 | 0.3 | 34.5 | 11.5 | 100.0 |
| Minimum | 0.0 | 0.5 | 0.5 | 0.0 | 0.0 | 0.0 | 0.0 | 0.0 | 0.0 | Tr | Tr | 2.5 | 25.2 |

TABLE A. 4
TEMPERATURES, LOS ALAMOS

| | Jan. | Feb. | Mar. | Apr. | May | June | July | Aug. | Sep. | Oct. | Nov. | Dec. | Annual |
|-------------|------|------|------|------|-----|------|------|------|------|------|------|------|--------|
| Av Max | 38 | 43 | 49 | 58 | 67 | 78 | 80 | 77 | 72 | 62 | 49 | 39 | 59 |
| Av Min | 16 | 21 | 25 | 33 | 42 | 50 | 54 | 53 | 47 | 36 | 26 | 18 | 35 |
| Extreme Max | 65 | 68 | 70 | 79 | 94 | 98 | 100 | 102 | 94 | 85 | 69 | 63 | 102 |
| Extreme Min | -9 | -14 | -3 | 8 | 24 | 31 | 43 | 42 | 27 | 17 | -4 | -2 | -14 |

APPENDIX B

GEOLOGY AND HYDROLOGY OF THE TA-35 SITE ¹

The following information was compiled from data collected during the course of ground-water investigations in cooperation with the Atomic Energy Commission.

The TA-35 site is located on a narrow mesa which separates Ten-Site Canyon and Mortandad Canyon (see Fig. 2.2.1 in the body of this report). Topographic relief in Mortandad Canyon is about 200 ft at a point due north of the Reactor Test Pit building, and in Ten-Site Canyon is about 120 ft due south of the building. The area is on the western half of the Pajarito Plateau which has been dissected into a number of finger-like mesas by eastward flowing, intermittent streams tributary to the Rio Grande. Mortandad Canyon and its tributaries drain the immediate area.

The TA-35 site is in the area investigated by the Geological Survey for a waste treatment plant. This part of the Pajarito Plateau is capped by the Bandelier Tuff of Pleistocene Age. The Bandelier is a welded rhyolite tuff consisting of crystal fragments, tuff breccia, and pumiceous material. The Bandelier is about 700 ft thick near TA-35. The base of the Bandelier was encountered at an altitude of about 6,380 ft at Test Well 8 in Mortandad Canyon, one mile east of

¹W. E. Hale, District Engineer, U. S. Geological Survey, Ground Water Branch, Albuquerque, New Mexico. Compiled by J. H. Abrahams and E. Baltz.

the site, which is at an altitude of about 7,200 feet. No bodies of water were found in the Bandelier at Test Well 8.

In the subsurface, the Bandelier Tuff is underlain by the Puye Conglomerate of Pliocene (?) Age. The Puye consists of silt, sand, and gravel composed of pebbles to boulders of volcanic rocks. Basalt flows are interbedded with Puye sediments in the eastern part of the Pajarito Plateau. Test Well 8 was drilled through 575 ft of the Puye Conglomerate, but did not reach the base of the formation. Water was not found in the upper part of the Puye, but was encountered in the lower part at a depth of about 985 ft below the floor of the canyon. The water rose about 25 ft in the well. This body of water, which is the main aquifer in the Los Alamos area, is at an altitude of about 5,960 ft in the vicinity of the site.

Studies indicate that little of the precipitation falling on the mesa tops filters into the Bandelier Tuff where it is overlain by soil. Probably clay in the alluvium in the canyons also inhibits or retards infiltration into the Bandelier. Data concerning the movement of water through tuff are scanty, but because the upper part of the Bandelier is moderately welded and jointed, some infiltration may occur along joints when water flows on bare rock. These joints commonly extend across and along the canyons.

Generally there is flow in Ten-Site and Mortandad Canyons only during spring snow-melt or during summer thundershowers. Radioactive liquids discharged accidentally would flow across the Bandelier Tuff for several hundred yards, then presumably infiltrate into the alluvium of Ten-Site or Mortandad Canyons. However, if the accident occurred during spring runoff or during a heavy summer thundershower, the wastes could be carried as a "slug" into Mortandad Canyon or conceivably to the Rio Grande. Observation wells already constructed in Mortandad Canyon below the mouth of Ten-Site Canyon would serve to monitor the liquids in the alluvium.

APPENDIX C

UCX NUCLEAR SAFETY SYSTEM

The sole purpose of the nuclear safety system is to initiate a fast, automatic scram. Three independent neutron flux measuring channels continually monitor the critical assembly. A trip or high flux level on any channel automatically scrams the assembly. A schematic diagram of the safety system appears in Fig. C.1., and each section of the system is described below. In the diagram, Sections I, II, IV, and V of channel 1 are shown in detail.

1. Section I

Section I of each channel incorporates the neutron ion chamber, chamber power supply, and electrometer circuit. The ion chamber delivers current, which is proportional to reactor power, to the input of the electrometer circuit. The electrometer is a current measuring device with two linear ranges. The voltage output equals 10 volts at 10^{-8} amperes current with S_1 open and 10 volts at 10^{-7} amperes with S_1 closed. The press-to-test switch introduces a current of 10^{-8} ampere. This feature allows each channel to be checked prior to an experiment.

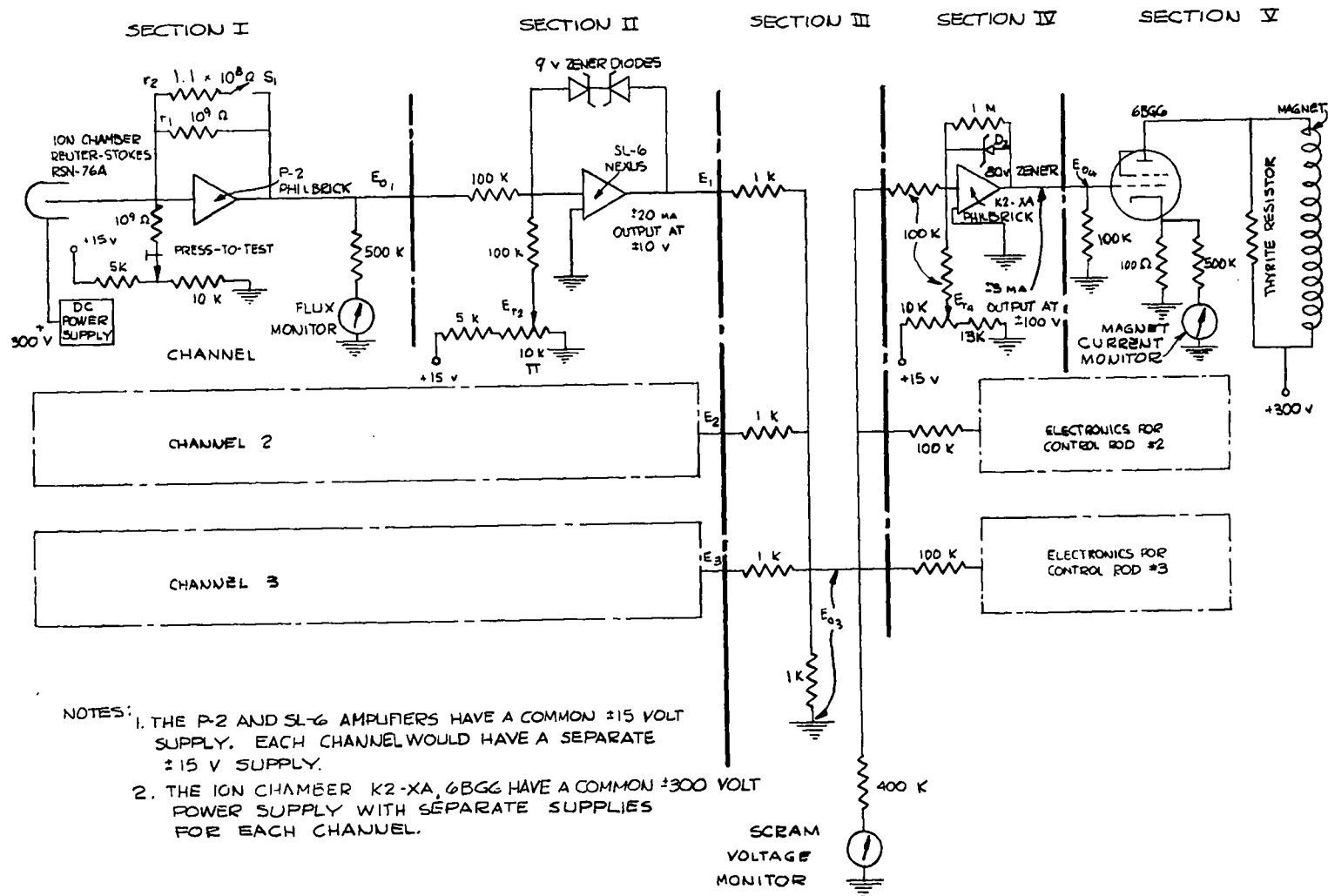


Fig. C.1 Schematic Diagram of UCX Nuclear Safety System.

2. Section II

Section II is a comparator circuit of each channel. The output of the electrometer circuit, E_{o_1} , is compared to reference voltage, E_{r_2} . When $|E_{o_1}| < |E_{r_2}|$ the comparator circuit's output is -9 volts. When $|E_{o_1}|$ becomes an infinitesimal amount (9 volts/ 5×10^5) greater than $|E_{r_2}|$ the circuit's output swings to +9 volts. The reference voltage, E_{r_2} , may be varied to compensate for differences in detector sensitivities and, therefore, will allow the scram levels of each channel to be set equal.

3. Section III

Section III is a passive adder. In this case it is used as a logic circuit. The output, E_{o_3} , varies according to:

$$E_{o_3} = \frac{(E_1 + E_2 + E_3)}{4} \quad (1)$$

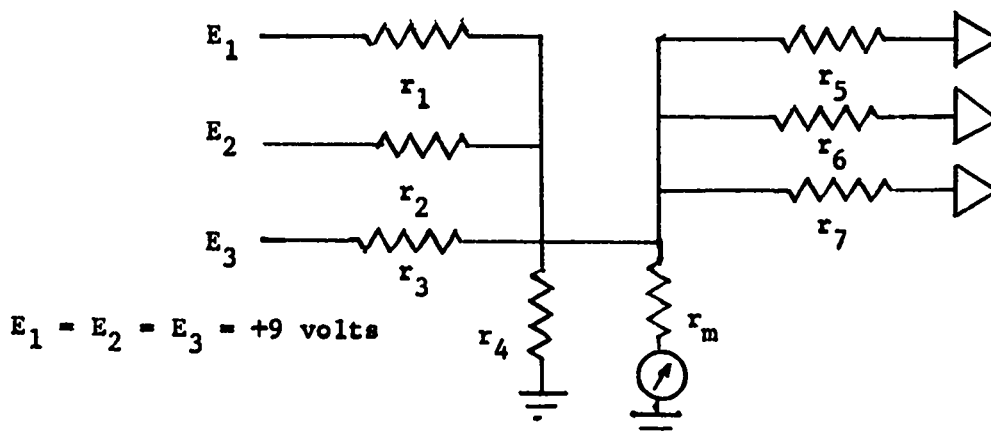
This expression is valid when E_1 , E_2 , and E_3 are low-impedance voltage sources. When E_{o_3} is not significantly loaded, high impedance voltage sensing of E_{o_3} is required.

E_{o_3} gives an indication of the status of the three flux measuring channels. Under normal conditions, according to equation 1, $E_{o_3} = -6.75$ v. A high flux at the ion chamber of any channel produces a +9 v input to the logic circuit. E_{o_3} rises to -2.25 v, and a scram is initiated. Whenever $E_{o_3} > -2.25$ v, the assembly is scrambled; therefore, a short or open circuit in any channel causes a scram.

The logic circuit is the common link in the safety system. An analysis of the effects of failures in the logic circuits and its associated components is presented in Table C.1. In every case the failure produces a safe effect.

TABLE C.1

Failure Analysis of Logic Circuit
and Associated Components



The following analysis assumes a single failure in the above network with all input channels having scram signals.

| <u>Failure</u> | <u>Scram Voltage*</u> |
|------------------------------|------------------------------------|
| $r_1, r_2,$ or r_3 shorted | + 9 volts |
| $r_1, r_2,$ or r_3 open | +5.17 volts |
| r_4 open | +9 volts |
| r_4 shorted | 0 volts |
| r_m open | Meter inoperative, no other effect |
| r_m shorted | 0 volts |
| $r_5, r_6,$ or r_7 shorted | 0 volts |
| $r_5, r_6,$ or r_7 open | +6.75 volts |

* Any voltage $\bar{>}$ -2.25 v will scram the reactor assembly.

4. Section IV

Section IV is made up of three DC amplifiers. These amplifiers are isolated from each other with 100 k resistors. A malfunction in one amplifier will not affect operation of the others. Each amplifier controls the bias potential to a pentode vacuum tube that delivers current to an individual rod magnet. A gain of ten is required to convert the relatively small voltage swing of the logic circuit to larger values for biasing the 6BG6 pentodes. Diode D_2 , an 80-v zener, insures that the amplifier does not saturate when E_{o_3} is $> +1.25$ v. E_{r_4} is adjusted to provide a 50 ma magnet current.

The output of each amplifier varies according to:

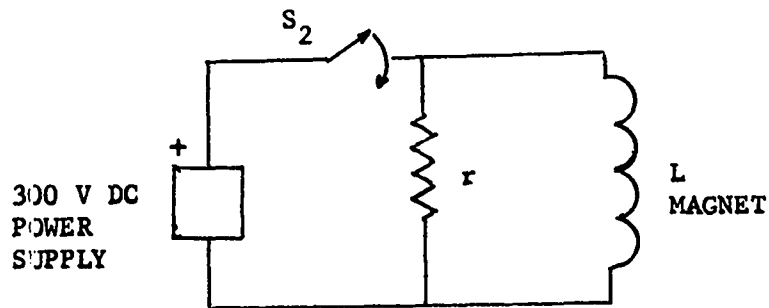
$$E_{o_4} = -10 \left[E_{o_3} + E_{r_4} \right] \quad (2)$$

The DC amplifiers use conventional analog computer circuits of proven reliability.

5. Section V

Section V contains power amplifiers that furnish current to each rod drive magnet. The 6BG6 power pentode is a rugged tube which will withstand high peak plate transient voltages of the sort that are generated when the magnet's current is interrupted.

The magnet has a 100-pound lift capability at 100 milliampere current. Quick release time is obtained by discharging the magnet's energy into a high impedance load, a thyrite resistor:



If S_2 is closed and then opened instantaneously, the current in the magnet will change according to:

$$I_m(t) = I_0 e^{-\frac{r}{L}t}$$

With respect to L , r must be large for the current to decay rapidly.

6. General Features

All safety circuits are mounted in one instrument rack and fed from a 115 v AC breaker reserved for these circuits. Failure of the safety system primary power supply produces a scram of the assembly.

Any of the direct current voltages in the safety system circuits can be connected, through a selector switch, to a meter mounted on the front of the chassis. Prior to each operation of the assembly, each voltage is checked.

A monitor on the power supply for the ion chamber of each safety channel is not necessary. These power supplies also serve as the source of current to the rod drive magnets. If a power supply fails, the magnet releases its rod.

APPENDIX D

HAZARD ANALYSES

1. Temperature Coefficients

To determine separately the fuel and moderator coefficients, cell calculations were performed using a multigroup "speed-up" code. In such calculations, the thermal energy region is divided into a number of separate energy groups. The group cross sections include both up scattering and down scattering possibilities, since, in the thermal region, neutrons may gain energy as well as lose energy in collisions with moderator nuclei. Evaluations were made of the shifts in thermal neutron spectra that occur whenever the fuel temperature increases while the moderator temperature remains constant. During heating of the fuel phase, both spatial and energy changes occur in the spectrum.

2. Reactivity Addition Excursions

In the analysis of transients in UCX, it is important to separate out the fuel and bulk moderator effects because thermal coupling between the two media is loose. For the present analysis, it was assumed, conservatively, that heat is transferred from the fuel to the bulk moderator by radiation only. Under these conditions, the fuel temperature rises quite rapidly during an excursion. Therefore, the negative fuel temperature coefficient is the principal mechanism that limits the extent of the power rise during the early stages of a

transient. A smaller but rapid shutdown mechanism, associated with direct heating of the bulk moderator, is also effective. The bulk moderator temperature rises as a result of the direct deposition of 5% of the fission energy by the slowing down of fast neutrons and attenuation of fission gamma ray energies in the moderator.

The following equations were used to describe transients in the UCX:

$$\frac{dN(t)}{dt} = \frac{[\rho(t) - \beta]}{\Lambda} N(t) + \sum_{i=1}^6 \lambda_i C_i(t) + S \quad (1)$$

$$\frac{dC_i(t)}{dt} = \frac{\beta_i}{\Lambda} N(t) - \lambda_i C_i(t) \quad i = 1, 2, \dots, 6 \quad (2)$$

$$\rho(t) = \rho(0) + \alpha_f [T_f(t) - T_f(0)] + \alpha_m [T_m(t) - T_m(0)] \quad (3)$$

$$C_f \frac{dT_f(t)}{dt} = Q_f BN(t) - K_r [T_f^4(t) - T_m^4(t)] \quad (4)$$

$$C_m \frac{dT_m(t)}{dt} = Q_m BN(t) + K_r [T_f^4(t) - T_m^4(t)] \quad (5)$$

where

$N(t)$ = neutron level

$C_i(t)$ = delayed neutron precursor level of the ith type

- $\rho(t)$ = reactivity
 $T_f(t)$ = fuel temperature
 $T_m(t)$ = moderator temperature
 β = total delayed neutron fraction
 β_i = delayed neutron fraction for the ith group of delayed neutrons

$$\sum_{i=1}^6 \beta_i = \beta$$

 λ_i = decay constant for the ith group of delayed neutron precursors
 S = independent source of neutrons
 Λ = prompt neutron generation time
 a = impressed reactivity ramp rate
 α_f = fuel temperature coefficient
 α_m = moderator temperature coefficient
 C_f = fuel heat capacity
 C_m = moderator heat capacity
 Q_f = fraction of fission energy deposited in the fuel
 Q_m = fraction of fission energy deposited in the moderator
 K_r = radiative heat transfer coefficient between fuel and moderator
 B = conversion factor between neutron level and power

Equations (1) to (5) were solved by successive expansion of $N(t)$, $C_i(t)$ $i = 1, \dots, 6$, $T_f(t)$, and $T_m(t)$ in Taylor series to order K about $t - t_j$:

$$N(t_{j+1}) = \sum_{n=0}^K \frac{N^{(n)}(t_j)(t_{j+1} - t_j)^n}{n!} \quad t_{j+1} > t_j$$

$$C_i(t_{j+1}) = \sum_{n=0}^K \frac{C_i^{(n)}(t_j)(t_{j+1} - t_j)^n}{n!} \quad \text{etc. (6)}$$

where $N^{(n)}(t_j)$ denotes the n th derivative of $N(t)$ evaluated at $t = t_j$.

To determine the time step $t_{j+1} - t_j$ the following criterion is applied

$$\frac{|N^{(K+1)}(t_j)| (t_{j+1} - t_j)^{K+1}}{N(t_j) (K+1)!} = \epsilon \quad (7)$$

where ϵ is an input parameter. Thus, the time step for each iteration is calculated from

$$t_{j+1} - t_j = \left[\frac{\epsilon (K+1)! N(t_j)}{|N^{(K+1)}(t_j)|} \right]^{\frac{1}{K+1}} \quad (8)$$

The derivatives occurring in Eq. (6) are obtained by successive differentiation of the system of coupled Eqs. (1) to (5) and evaluating these derivatives at $t = t_j$.

This approximate method has been compared with analytic solutions in a few special cases where such solutions exist. The accuracy of the approximate method was found to be very satisfactory for $\epsilon = 10^{-6}$ and $K = 4$.

Below are listed the various constants used in the two calculations described in Sec. 6.2.

Cases I and II

$$\begin{aligned} \epsilon &= 10^{-6} \\ a &= 5\text{¢/sec} \\ K &= 4 \\ C_f &= 0.3 \text{ Mw-sec/}^\circ\text{C} \\ \Lambda &= 1.14 \times 10^{-3} \text{ sec} \\ C_m &= 12 \text{ Mw-sec/}^\circ\text{C} \\ Q_f &= 0.925 \\ \alpha_m &= -2.3 \times 10^{-4} \text{ k/}^\circ\text{C (3.64/}^\circ\text{C)} \\ Q_m &= 0.075 \\ K_r &= 6.37 \times 10^{-13} \text{ Mw/}^\circ\text{k}^4 \\ \alpha_f &= -2.6 \times 10^{-5} \text{ k/}^\circ\text{C (0.41¢/}^\circ\text{C)} \\ B &= 1.541 \times 10^{-14} \text{ Mw} \\ S &= 200 \text{ neutrons/sec (inherent source)} \\ \beta_1 &= 2.1 \times 10^{-4} & \lambda_1 &= 1.244 \times 10^{-2} \text{ sec}^{-1} \\ \beta_2 &= 1.4 \times 10^{-3} & \lambda_2 &= 3.051 \times 10^{-2} \\ \beta_3 &= 1.26 \times 10^{-3} & \lambda_3 &= 1.1144 \times 10^{-1} \\ \beta_4 &= 2.53 \times 10^{-3} & \lambda_4 &= 3.0137 \times 10^{-1} \\ \beta_5 &= 7.4 \times 10^{-4} & \lambda_5 &= 1.1363 \\ \beta_6 &= 2.7 \times 10^{-4} & \lambda_6 &= 3.0137 \end{aligned}$$

Case I

$$\rho(0) = -2.5 \times 10^{-2}$$

Ramp terminated after 90¢ excess reactivity had been added,
i.e., 96.125 sec after the start of the 5¢/sec ramp.

Case II

$$\rho(0) = 0$$

Ramp terminated after \$4 excess reactivity had been added,
i.e., 80 sec after the start of the 5¢/sec ramp.